

UNIVERSITY OF PADUA  
DEPARTMENT OF GEOSCIENCES



Master's Degree Course in Geology and Technical Geology

MASTER'S DEGREE THESIS

Comparing the MAT 252 and Delta V Advantage mass spectrometers  
for stable O and C isotopes analyses. A case study from the lower part  
of the PCS sediment core (Lower Pleistocene, Calabria, Italy)

Supervisor: Prof. Luca Capraro

Co-rapporteur: Dr. Elena Zanola

Undergraduate: Wei Lin  
Serial number: 2057886

ACADEMIC YEAR: 2022/2023

## TABLE OF CONTENTS

Introduction	
1. A study case: the lower part of the PCS sedimentary core (Lower Pleistocene, Calabria, Italy)	
1. 1 PCS core	
1. 2 The Mediterranean Sea	
1. 3 Geology of the study area	
1. 4 Stratigraphy of the study area	
2. Pleistocene	
2. 1 Chronostratigraphy	
2. 2 Climate and ice ages	
2. 3 Orbital theory of ice ages	
3. Stable isotopes	
3. 1 Introduction to stable isotopes	
3. 2 Isotope fractionation	
3. 3 Oxygen stable isotope	
3. 4 $\delta^{18}\text{O}$ and reconstruction of past climate	
3. 5 Carbon stable isotopes	
3. 6 $\delta^{13}\text{C}$ in the ocean	
4. Foraminifera	
4. 1 Biological characteristics	
4. 2 Applications in Paleoceanography	
4. 3 Benthic foraminifera	
4. 4 <i>Uvigerina peregrina</i>	
5. Materials and methods	
5. 1 Brief introduction	
5. 2 Pre-pick preparation	
5. 3 Picking	
6. Mass spectrometer	
6. 1 Brief introduction	
6. 2 Mass spectrometer experiments by the University of Padova (using the Delta V Advantage)	
6. 3 Mass spectrometer experiments by Reghellin in 2010 (using MAT 252)	
7. Result and Discussion	
7. 1 $\delta^{13}\text{C}$ curve and comparison	
7. 2 $\delta^{18}\text{O}$ curve and comparison	
7. 3 Further discussion	
8. Conclusion	
Table	
Acknowledgements	
References	

## Introduction

The Delta V Advantage and the much more expensive MAT 252 mass spectrometers are commonly employed worldwide for the analysis of “light” stable isotopes, such as carbon and oxygen. However, the consistency of the results produced by these instrumentations has been poorly tested, especially in the case of daily routinary use.

In order to explore the differences in the acquisition of isotope data by these two different mass spectrometers, we propose as a case study a stable isotope analysis on benthic foraminiferal tests from the lower part of the PCS sedimentary core (Lower Pleistocene, Calabria, Italy), where the Geosciences Department of Padova has been studying for more than ten years, focusing the research mainly on analysing the biostratigraphic and geochronological context of these deposits. The comparison was investigated on two separate occasions using the mass spectrometers mentioned above. In either case, samples were washed, sieved, and cleaned following identical procedures, which ensured consistency while performing the analyses. A continuous record for  $\delta^{18}\text{O}$  and  $\delta^{13}\text{C}$  was reconstructed using the Delta V Advantage mass spectrometer at the Department of Geosciences of the University of Padova, which was compared to that obtained in 2010 by Reghellin for the very same stratigraphic interval using the MAT 252 mass spectrometer of the Department of Geology of the University of Stockholm (Sweden). At the same time, our experiments at the University of Padova have higher resolution data than the previous Reghellin experiments, with  $\delta^{18}\text{O}$  and  $\delta^{13}\text{C}$  values reaching nine decimal places and sampling every 0.1 m. High-resolution sampling and supplemented by information from previous studies of the area provide us with good conditions for comparing data from two different spectrometer results.

1. A study case: the lower part of the PCS sedimentary core (Lower Pleistocene, Calabria, Italy)

### 1. 1 PCS core

The PCS core was retrieved by Professor Capraro *et al.* in 2010 and is currently stored at the Department of Geosciences. It is an about 90 m long sediment core which recovered near the Crosia (CS) village in Ionian Calabria (Southern Italy), allowing the recovery of a stratigraphic record of the lower Pleistocene. The objective of its drilling was to allow the recovery of a critical part of the local stratigraphy for which no outcrop has been recorded, by means of tracing a couple of distinctive key beds (i.e., the so-called “Cristina bed” and “Ledro laminite”; Segalla, 2007). PCS core mainly consists of a succession of sands and pelites, covering almost the entire stratigraphic succession of the Crosia-Calopezzati sedimentary basin. However, it should be noted that as the PCS core did not reach the basal sandy unit, it could document only part of the vertical transition (from coastal to the outer shelf and upper slope facies). (Reghellin, 2010)

After photographic documentation and some sample pre-processing by the Department of Geosciences of the University of Padova, 120 samples were selected for the -47m to -87m (core depths are referred to the ground level) portion of the PCS core, and labelled as PCS 1 - PCS 121. After that, these samples were transported to the Department of Geological Sciences of Stockholm University and analysed by a Finnigan MAT 252 isotope ratio mass spectrometer (IRMS) after a series of pre-picking and picking steps for the foraminiferal specimen. Based on the isotope data obtained from MAT 252 IRMS, Reghellin had reconstructed a stable carbon and oxygen isotopic record for the benthic foraminiferal species *Uvigerina Peregrina*.

To realize the following comparison, our samples were taken from -50.0m to -76.2m of PCS core, largely consistent with the depths at which the samples (i.e., -47.0m (PCS 1) - -87.0m (PCS 121)) were studied by Reghellin. A continuous record for  $\delta^{18}\text{O}$  and  $\delta^{13}\text{C}$  was reconstructed using the Delta V Advantage mass spectrometer at the Department of Geosciences of the University of Padova.

### 1. 2 The Mediterranean Sea

The Mediterranean Sea is located in the middle latitudes and has unique climatic characteristics (called the Mediterranean climate), with strong contrasts in winter and summer for most of the basin, which means warm and dry conditions during summer while mild and rainy in winter. The strong seasonality and continuous input of sediments from the basin margin make the Mediterranean stratigraphic record one of the world’s best paleoenvironmental and paleoclimatic archives. Also, the small-sized basin allows protection and preserves the global climatic signal. The Mediterranean is a “soundboard” of what happens at the global scale, mainly from the climatic point of view, e.g., changes in sedimentary, circulation and production. These effects are mainly represented in the small basins, especially the Mediterranean, where the effects of changes are emphasized greatly with respect to the open ocean (which tends to buffer). In the Mediterranean, the small-scale and

mid-scale changes are incredibly well documented in the stratigraphic succession, especially in southern Italy, which makes it has enormous importance for the whole system study, in terms of climatic and chronostratigraphic points (e.g., the youngest part of the chronostratigraphic scheme was developed in the Mediterranean). As a landlocked basin, the Mediterranean basin is surrounded by the mainland and extends from east to west. It is connected with the open ocean in the Gibraltar Strait that separates Europe from North Africa since the end of the Miocene. Before that, the Gibraltar Strait was not the connection point; the main linkage between the Mediterranean and the open ocean (Indian Ocean) was located in the east region. This reversal of the connection point with the open ocean also has led to a dramatic change in the Mediterranean circulation.

Bathymetry in the Mediterranean is variable; large areas are characterized by shallow water, especially true in the northern part of the Mediterranean, i.e., the Adriatic Sea, where the water column is only a few meters thick; at the same time, there are areas which have more significant depths, the maximum depth in the Mediterranean is in the order of 5,700m, corresponding to the deepest part is located in the Eastern basin. From a topographic point of view, there are complex conditions with these considerable depth changes even at short distances. For example, in the area between Sicily and North Africa, the terrain suddenly sinks from an exceptionally shallow to an abyssal place in the middle of the Tyrrhenian Sea. These also reflect in the circulation pattern in the basin.

For convenience, the Mediterranean is divided into different small sub-basins. The Western basin and the Eastern basin are separated by the central Mediterranean and connected by the natural Sicily Channel (about 330m deep) between Sicily and Tunisia. Meanwhile, in the Mediterranean basin, two other smaller basins that are elongated along north-to-south distribution, namely the Aegean and the Adriatic, where are characterized by shallow and narrow water. The Ionian Sea, which develops southeast of Italy, is the deepest part of the Mediterranean, elongating eastward and reaching the Eastern Mediterranean coast. The Mediterranean basin also has two narrow and shallow straits: the Sicily Strait and the Gibraltar Strait. The former is the natural division between the Eastern and Western basins; the latter represents the closest part of the Mediterranean to the open ocean; this section is immediately affected by the incoming Atlantic waters after they have crossed the Gibraltar Strait.

On the sea surface, we can observe the interaction between the ocean and the atmosphere, as well as the interaction between the sea and the mainland. The Mediterranean is an evaporation basin, where the total amount of precipitation and runoff is less than the evaporation, characterized by just a few rivers that can effectively discharge fresh water into the basin. Therefore, the Mediterranean still persistently needs water inflow from the Atlantic and the Black Sea. E.g., the inflow of Atlantic surface waters (AW), which is cold and little salty. In exchange, the Mediterranean spill-out is the Mediterranean Outflow (MO), a deep, relatively warm and salty water mass, rich in nutrients, which enters the intermediate Atlantic dominion. Due to its distinctly unique characteristics from normal oceanic waters,

we can identify the presence of this water mass in the intermediate domain of a large part of the North Atlantic. Main fresh water inputs are provided by the northern part of the basin (i.e., the European side); of these, Po River and Drin River are the most effective. The basin's southern part is virtually significant only regarding the Nile River.

The salinity in the Mediterranean is extremely high on the sea surface and shows a strong gradient between the western and eastern sides. The lowest salinity is observed on the Atlantic side, and the Gibraltar Strait works as a barrier, dividing the open ocean where salinity is low and stay in normal values (ca. 35‰) and the Mediterranean, where salinity soars up to 39‰ in the eastern part.

Since the Mediterranean is a small basin compared to the ocean, it gets many complications (articulated in terms of geography and topography) in the distribution of the water masses. The following are the main water masses in the Mediterranean Sea.

Surface water mass (waters that reside at the top of the water column):

MAW (Modified Atlantic Waters), the waters given by the Atlantic to the Mediterranean. As we said before about the change in salinity from west to east, once the Atlantic water enters the Mediterranean, it virtually immediately begins to transform, including the growth of salinity and temperature over very short distances. As a result, the original Atlantic water is modified in time and space. This flow is virtually undisturbed until it reaches the Sicily channel, and MAW will break up into three main mid-branches in this confined small space. The first branch takes a northward trajectory, flowing along the western coast of Italy, and then enters the Lion's Gulf, becoming trapped by other surface flows occurring there, finally evolving into an anti-clock rotation. This tributary is also referred to as TSW (Tyrrhenian Surface Waters). The second branch deflects south, following the coast of North Africa, landing on the Sirte Sea and becoming a clockwise rotation there. The third part of the MAW flow can keep on the eastward movement but be squeezed when it passes the Sicily channel. The confined shallow channel induces the acceleration of this branch, which turns into the mid-Mediterranean Jet that can rapidly cross the Ionian Sea and reach the easternmost coast of the Mediterranean. Meanwhile, the jet current has another secondary branch which tries to reach the northern part of the Mediterranean basin and enter the Adriatic Sea and Aegean Sea. However, the surface water fluxes from these two regions (ASW and AeSW) provide a push to the secondary branch of the mid-Mediterranean Jet and make it move southward until it joins the main branch.

ASW (Adriatic Surface Waters) are the generation of surface water in the Adriatic; they are the only water mass that can reside in the north Adriatic area, which has exceptionally shallow space that can only hold one water mass. However, there is more space when ASW move north to south. The middle part of the Italian Peninsula corresponds to the middle Adriatic depression, which generates a depth of accommodation space in the order of 1,500m in very short distances, resulting in a sudden thickening of the water column. Also, another giant "step" is at the boundary between the southern Adriatic and the open Ionian Sea.

LSW (Levantine Surface Waters) reside in the eastern part of the Mediterranean and characterize the Eastern basin. This water mass generates when the mid-Mediterranean Jet reaches the Levantine coast and is forced to change the original direction. Following the local topography, the velocity of this flow also becomes increasingly slowed down with the direction changes. Also, during this water mass flows into the easternmost part of the Levantine basin, the water surface becomes warmer and saltier; up to this point, the character of the Atlantic water has completely disappeared, and this water mass is identified as LSW. After that, LSW will try to get back and cross the Sicily Strait; in this trajectory, however, the ASW and AeSW (Aegean Surface Waters) will disturb the current and push it southwards. Lastly, LSW meet the mid-Mediterranean Jet, which has more energy; with the friction between these two water masses, the LSW are pulled toward the original position, forming a closed circulation circuit.

Intermediate water mass (waters that reside in the middle of the water column):

EMOW (Eastern Mediterranean Overflow Waters) can flow out to the Western basin through the Sicily Channel. They are critical for the survival of all Mediterranean, derived from the mixing of LIW with the ADW (Adriatic Deep Waters) and AeDW (Aegean Deep Waters).

LIW (Levantine Intermediate Waters), the most significant intermediate water mass, reside in the Levantine basin, characterized by an excessively warm and salty surface. Conditions in the Levantine Sea change dramatically during the year because of the seasonal contrast between winter and summer, except for the amount of salinity preserved in this basin. During the summer, LSW persistently flow at the sea surface with a small density as the water still is warm and salty (39‰ and 28°C, respectively). When the wind blows from the north in winter, it causes the sea level temperature drops significantly (approximately from 28°C to 15°C). The densification of surface water generates the LIW, which provide an amount of water extended over the whole Mediterranean. The LIW do not reach the sea bottom and reside at 150 to 600m depth, as they are relatively "light" (low temperature but high salinity). Having similar densities to ADW and AeDW, they can be mixed afterwards and sink together; at this point, LIW can enter the Adriatic Sea and part of the Aegean Sea, while during the summer, LIW only can flow below the shallow domain toward the Gibraltar Strait due to the thermocline stratification.

Deep water mass (waters that reside at the bottom of the water column):

WMDW (Western Mediterranean Deep Waters). Basically, we can subdivide the deep Mediterranean domain into two main groups of deep waters: Western Mediterranean Deep Waters (WMDW) and Eastern Mediterranean Deep Waters (EMDW). WMDW are a widespread water mass that is continuously forming and residing in the deep part of the Western basin and sustains life in the basin because the continuous generation brings and conveys oxygen and other important survival requirements from the surface to the deeper part of the Western Mediterranean.

EMDW (Eastern Mediterranean Deep Waters) are the merger of Adriatic Deep Waters (ADW) and Aegean Deep Waters (AeDW). Analog to the generation of the LIW, they are induced by winds which are the Burian (Adriatic) and Vardar

(Aegean). Winter sea surface temperatures are forced to 12°C, thus compensating for the local waters with low salinity. In this case, the process is only triggered by the temperature gradients. The difference concerning EMDW is that they do not form by the direct sinking of surface waters, but upon mixing with the LIW (which are much saltier) to form super-dense waters. Therefore, LIW rule the dynamics of the Mediterranean.

TDW (Tyrrhenian Deep Waters) reside in the Tyrrhenian Sea. Because our study focuses on the eastern part of the Mediterranean, their details are omitted here.

ADW (Adriatic Deep Waters) are unexpected flows because the basin they are located in is very shallow, yet the generation of deep waters is in such a thin water column. They are similar to LIW in terms of deepening waters, which have strong seasonal contrast in temperatures. During the winter, the temperature of the Adriatic Sea's surface drops even more significantly than in the Levantine Sea; besides the effectiveness of the wind, there is also a lot of river runoff which provides cold waters flowing from the continents. As a result, both the temperature and salinity (The dilution of surface water due to the river runoff and continuous input of the Black Sea) of the seawater drop, generating deep waters that are typical of the shallow basin, i.e., ADW.

AeDW (Aegean Deep Waters) have conditions similar to ADW and generate at the interface between the Aegean Sea and the Ionian Sea.



Figure 1.2.1: Trajectory of major water masses (MAW, LIW and AdDW) in the Mediterranean at an approximate scale (from Capraro, 2019).



### 1.3 Geology of the study area

The Calopezzati-Crosia area has already been the subject of some studies (e.g., Segalla, 2006; Reghellin, 2010; Gozzer, 2011) that have made it possible to frame the sedimentary succession in a relatively well-defined chronological and tectonic stratigraphic context.

Our study area is located at the base of the northeastern slope of the Sila Massif, along the Ionian coast of northern Calabria (Fig. 1.3.1), which is characterized by the absence of cliffs and a slope that descends gradually towards the sea. The Sila massif (also Serre and Aspromonte massifs) is part of the Calabrian Arc (Fig. 1.3.2). This complex orogenic chain crosses the region longitudinally, with a northeast-southwest direction. It is made up of tectonic units that overlapped from the Lower Cretaceous to the Palaeocene with a European vergence, which in turn overlapped, starting from the Lower Miocene, on the Apennine chain being formed (Gasperi, 1995). The area is bordered to the west by the Trionto River, while to the north, it is cut by the coastline, which shows a northwest-southeast trend conditioned by tectonic fault lines (Van Dijk and Okkes, 1991). Subsequently, during the mid-Pliocene phase, the Alpine and Apennine welded together and overlapped eastwards on the foreland deposits (Carobene, 2003).

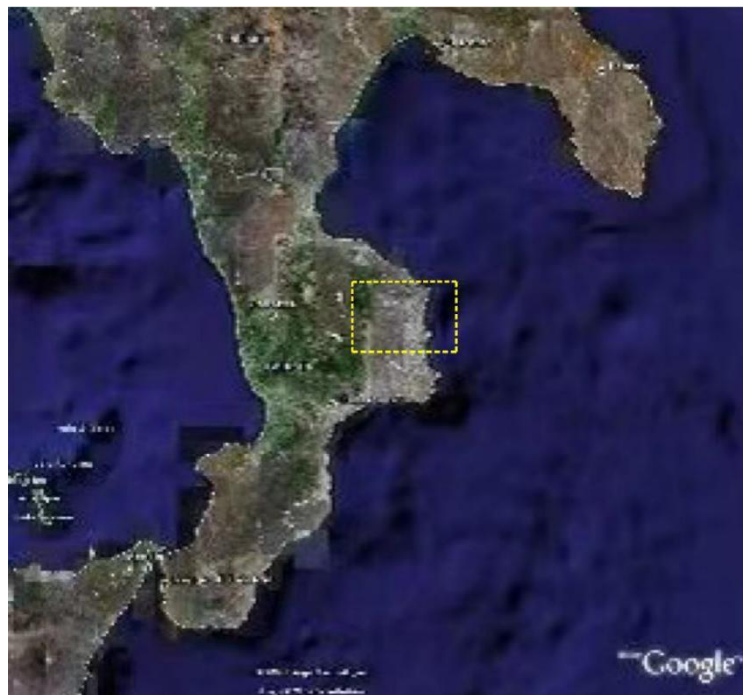


Figure 1.3.1 The study setting (yellow dashed grid).

Unlike the Apennines, the Calabrian Arc is almost entirely composed of crystalline metamorphic rocks. It comprises north-eastern nappe that previously belonged to the African block. The Calabrian Arc and the Apennine chain are separated by a shear zone that extends with a direction approximately east-west immediately below the limestone massif of the Pollino.

The Calopezzati-Crosia area is located between the south of the Crotona Basin (Late Neogene) and the coeval Crati Basin, to which the Rossano sub-basin belongs to the north (Ogniben, 1962). These basins both lie above the Calabrian

accretionary wedge, the inner part of which was characterized by a significant distensive phase during the Middle and Upper Pliocene (probably associated with the opening of the south-western Tyrrhenian) followed by a compressional phase during the Lower Pleistocene (Van Dijk, 1992 and 1993; Sheepers, 1994). Subsequently, during the Middle Pleistocene, regional tectonics was characterized by a stress release phase with transpressional tectonics, the rupture of the subduction slab and the beginning of an isostatic settlement phase (Van Dijk and Okkes, 1991; Van Dijk 1992 and 1993; Sheepers, 1994; Van Dijk and Sheepers, 1995). These conditions led to a general uplift of the area (Massari et al., 2001).

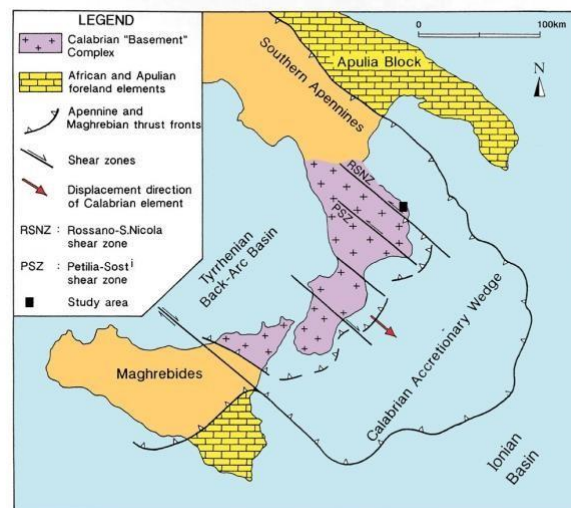


Figure 1.3.2: Structural map of Southern Italy (from Massari et al., 2002) and the location of the study area (solid black square).

#### 1. 4 Stratigraphy of the study area

The stratigraphic succession of the study area is described as follows (Segalla, 2007), from base to roof (Fig. 1.4.1):

- Messinian basal complex
- Yellowish sandstones (Pliocene - Lower Pleistocene)
- Clayey marls with laminites and cinerites (Lower-Middle Pleistocene)
- Regressive sandstones (Middle Pleistocene)
- Marine terraces (Middle-Upper Pleistocene)

The three-dimensional analysis of the lithology exposed in the Crosia-Calopezzati area allows the tectonic and eustatic evolution of the basin to be reconstructed (Segalla, 2006; Reghellin, 2010; Gozzer, 2011).

The basal part of the local sedimentary sequence is characterized by the presence of a transgressive systems tract (TST) followed by a highstand systems tract (HST). The highstand deposits appear to be truncated by an erosional surface correlated with a regressive systems tract (RST), on which rest marine terraces of four different orders that originated during the fall of the local sea level before the final emersion of the area (Carobene, 2003; Gozzer, 2011). The transgressive phase is plausibly related to the tremendous extensional phase that plagued this sector

during the Middle and Upper Pliocene; at the same time, the final regression follows a tectonic uplift phase that began during the Middle Pleistocene. This phase of forced regression was repeatedly interrupted by episodes of rise in relative sea level, leading to the formation of various orders of marine terraces (Gozzer, 2011). At a stratigraphic point, the oldest deposits that outcrop in the study area consist of well-cemented quartzose-feldspathic sandstones, the age of which is commonly referred to as the Messinian (Upper Miocene; Carobene, 2003). These deposits constitute the substratum of the Plio-Pleistocene marine succession, which in turn is characterized by thicknesses ranging from approximately 60m in the southern portion of the area to over 250m in the northern part (seaward). The latter datum was obtained from wells dug to search for water for agricultural use in the municipality of Crosia (Gozzer, 2011).

The Pleistocene succession consists predominantly of pelitic deposits confined at the base and roof by sandy bodies representing the transgressive and regressive parts of the succession, respectively. The thickness of the intercalated clay unit thus shows a gradual decrease in a north-south direction. Outside the Crosia village, the two sandy bodies are separated only by a thin layer of clayey siltstones, while the pelites are largely dominant towards the sea. Rapid facies variations over short distances are also observed in the transversal direction, orthogonal to the axis of the basin, with the presence of massive slumping at its margin that seems to indicate that the Crosia-Calopezzati basin was a small gulf, narrow and elongated, with very steep edges (Gozzer, 2011).

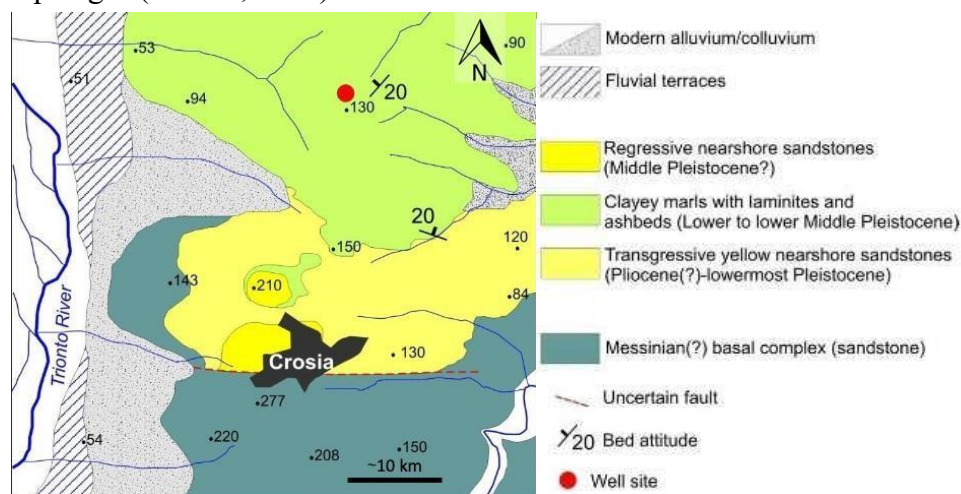


Figure 1.4.1: Simplified geological map of the Crosia sector (approximate scale) with the main units identified in the area and the location of the PCS core drilling site (red circle) (from Gozzer, 2011) .

## 2. Pleistocene

### 2. 1 Chronostratigraphy

The second Quaternary Conference in 1932 established the division of the Pleistocene into Early, Middle and Late stages. In 1948, the IUGS (International Union of Geological Sciences) recommended the Villafranchian (Italy) as the boundary between the Pleistocene and the Pliocene. The absolute age of the Villafranchian was determined to be 1.6 - 1.8 Ma. In 1977, the International Union

for Quaternary Research (INQUA) recommended the Vrica section in Italy as the lower base of the Pleistocene, with an absolute age of about 2.5 Ma. There are also proposals to date the Pleistocene lower boundary to 3.3 - 3.5 Ma, with reference to the paleomagnetic divide between the Gauss normal and Gilbert reversed polarity chron.

Until 1984, the Plio-Pleistocene boundary was formalized for the first time by the International Commission on Stratigraphy (ICS), following the previous INQUA proposal to define the bottom in the Vrica section (Crotona, Calabria), while the age of the boundary was astronomically tuned at ca. 1.81 Ma (Lourens *et al.*, 2004). This defined boundary was determined as a GSSP (Global Stratotype Section and Point) and available to the scientific community worldwide for over 20 years.

## 2. 2 Climate and ice ages

The Pleistocene was a time of dramatic climatic change on Earth and had active glacial action referred to as the Glacial Epoch by E. Forbes in 1846. Large-scale glacial activity occurred during this period in the high and mid-latitudes of the northern hemisphere, as well as in some high mountains in the lower latitudes. At the peak of several Pleistocene ice ages, more than 30% of the global land area was covered by glaciers. The progression and receding of glaciers created numerous alternations between cold ice ages and warm interglacial periods. It led to significant sea level rise and fall, shifts and upheavals in climate zones, and the migration or extinction of plants. These events had a significant impact on the development of early human cultures. As a result, many scholars have advocated using the ice age sequence as the primary criterion for Pleistocene staging.

Based on the  $\delta^{18}\text{O}$  record curves reconstructed by scientists in different settings of the world, it shows that the Lower Pleistocene was dominated by shorter cycles with a 40-kyr cyclicality (corresponding to the obliquity cycle, which we will discuss in the next section), while beginning from MIS 25 (ca. 1 Ma) cycles are longer, showing a ca. 100-kyr period (corresponding to the eccentricity cycle). According to mathematic modelling, it is likely that eustatic oscillations were in the order of 40 - 60m during the Lower Pleistocene (Raymo *et al.*, 1989) and about 100m during the Middle and Late Pleistocene (Shackleton, 1987).

## 2. 3 Orbital theory of ice ages

In 1930, Milankovitch postulated that wobbles in Earth's orbit changed the distribution of solar energy on the planet's surface, pushing Earth into or out of an ice age. There are three main orbital cycles involved (Figure 2.3.1):

1. Eccentricity: the ellipse of orbit around the sun changes every hundred thousand years (100-kyr cycle).
2. Obliquity: the angle of intersection of the Earth's ecliptic and equator changes by one cycle of about 41 kyr.
3. Precession: larger impact on lower latitudes. Defined as the cycle of changes in the Earth's rotation axis progression, which was about 21.7 kyr.

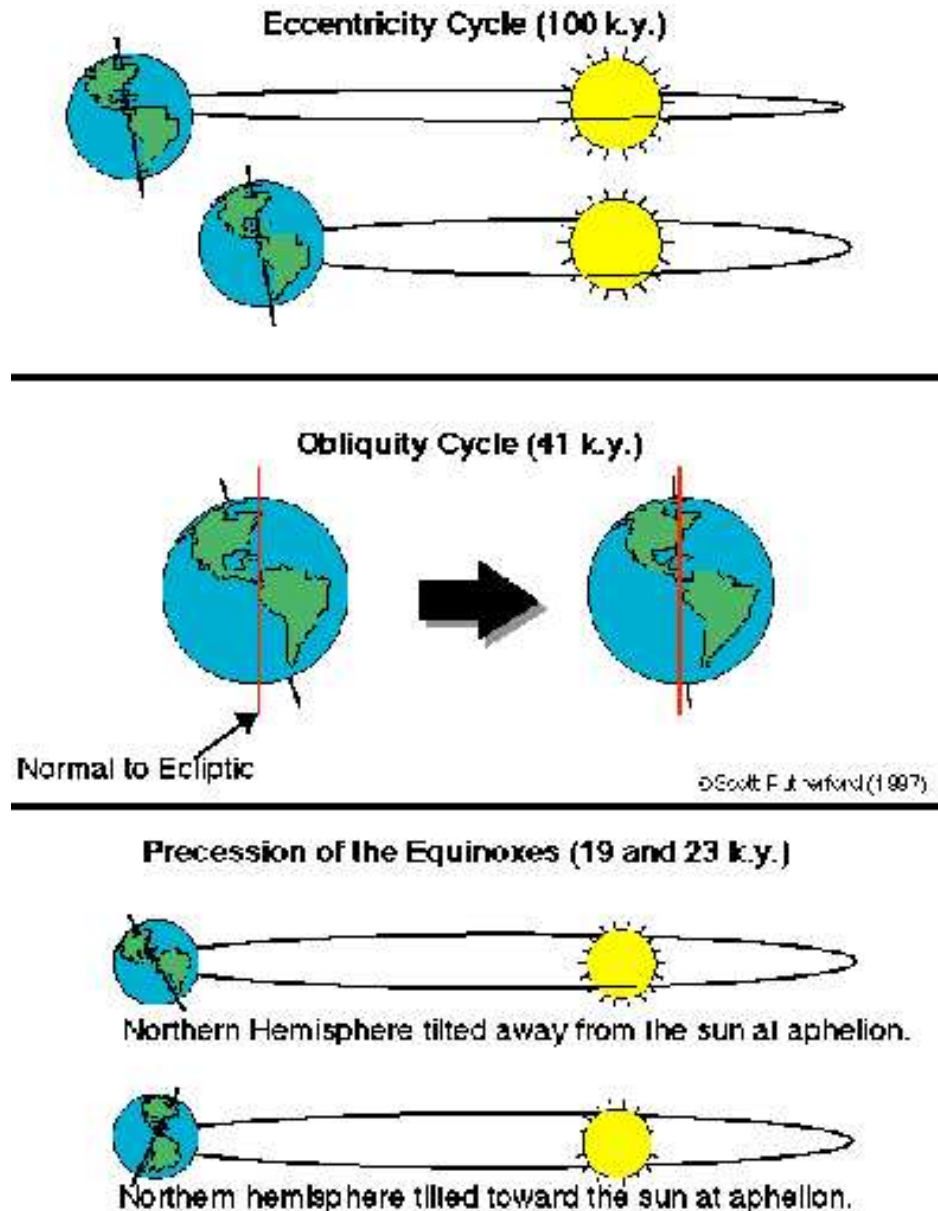


Figure 2.3.1: three main orbital cycles: eccentricity cycle, obliquity cycle and precession of the equinoxes (from S. Rutherford, 1997).

These orbital cycles play together, and we can calculate the half-year mean insolation at  $65^{\circ}\text{N}$  for the last 600 years. Meanwhile, for questions: what configuration of the Earth's orbit is favourable for the emergence of ice age climates? Milankovitch gave the answer that a decrease in the tilt of the Earth's axis and the presence of the Earth at aphelion in the Northern Hemisphere during the summer would favour the occurrence of an ice age climate. It can be seen that such a configuration of orbital elements would correspond to a reduction in the amount of solar radiation in the Northern Hemisphere at high latitudes in summer. Thus, Milankovitch's theory can be summarized as follow: changes in summer solar radiation around  $65^{\circ}\text{N}$  were the main driver of the Quaternary ice age cycle (Milankovitch, 1941).

However, when the theory was introduced, it was met with much scepticism until

1955, when Emiliani published a paper about the temperatures of Pacific bottom waters and superficial polar waters during the Tertiary (Emiliani, 1955). By using the test of benthic foraminifera to get the oxygen isotope ratio, Emiliani determined that three deep-sea temperatures had declined from 10.4 to 7.0 to 2.2°C across epochs and found that they were consistent with abundant geological and paleobotanical evidence for global cooling during the Cenozoic. With a 700m long core from the Caribbean, Emiliani obtained the first view of the glacial cycles from oxygen isotopes based on the surface temperature from planktonic foraminifer species and labelled the *Marine Isotope Stages* (MIS) on the acquisition curve. A significant discovery followed: the ages of the even core stage (i.e., ice stage) from Emiliani's research match the ages of insolation minima collected by Milankovitch. Thus, Emiliani supported the orbital theory of the ice ages by Milankovitch. However, geologists must have an accurate chronology of the Late Pleistocene climate for the last 900 years to prove this theory. Since then, scientists have tried to reconstruct the paleoclimate using different indicators (we will refer to them later), constantly adding to and strengthening this theory.

### 3. Stable isotopes

#### 3.1 Introduction to stable isotopes

Isotopes are atoms with the same number of protons and different neutron numbers that occupy the same position in the periodic table of the elements. For example, carbon has several isotopes, including  $^{12}\text{C}$ ,  $^{13}\text{C}$  and  $^{14}\text{C}$  (which are radioactive). The chemical behaviour of the isotopes is almost identical. However, the atomic weights or mass numbers are different. Thus their mass spectral behaviour, radioactive transitions and physical properties (e.g., diffusion instincts in the gaseous state, vapour pressure, boiling and melting point) differ. Differences in the number of protons and neutrons can affect the stability of the isotope's nucleus. Therefore, isotopes can be categorised as stable isotopes and radioactive isotopes.

Stable isotopes are atoms of the same element that are relatively stable in their physical properties and free from radioactivity and radiation effects. They involve natural, non-radioactive isotopes that concur with both inorganic and biological cycles. At present, more than 300 such isotopes are found, while the other isotopes are unstable or radioactive. In general, stable isotopes with lower atomic masses are more abundant than their larger counterparts; thus, only one isotope (i.e., the lower atomic masses one) dominates, with the others present in trace amounts.

In geological applications, radioisotopes are often used for dating, contributing the ability to calibrate events in Earth's history to absolute time as an integral partner in the effort of constructing the geologic time scale (Gradstein *et al.*, 2012), while stable isotopes are critical to paleoclimate and paleoenvironmental studies, mainly focus on isotopic variations attributed to mass-dependent isotopic fractionation. Among all stable isotopes, hydrogen ( $^1\text{H}$ ;  $^2\text{H}$ ), carbon ( $^{12}\text{C}$ ;  $^{13}\text{C}$ ), oxygen ( $^{16}\text{O}$ ;  $^{18}\text{O}$ ) and sulphur ( $^{32}\text{S}$ ;  $^{34}\text{S}$ ) stable isotopes are particularly important to geological study because of their involvement in rock and mineral formation, the hydrological cycle and biological processes (Bigeleisen, 1965). And, since the magnitude of



differences brought about by isotopic substitution in the physical and chemical properties of atoms and molecules (i.e., isotope effects) is proportional to the relative mass difference between isotopes, significant isotopic variations in nature are also limited to these light elements (Anderson *et al.*, 1983).

To measure the relative concentrations of different isotopes (e.g., O or C), mass spectrometers are used. They separate gaseous isotopic molecules based on their mass. E.g., for measuring O and C in calcite, the latter must be converted to CO<sub>2</sub>:



The mass of CO<sub>2</sub> isotopic molecules may range between 44 (<sup>12</sup>C<sup>16</sup>O<sup>16</sup>O) and 49 (<sup>13</sup>C<sup>18</sup>O<sup>18</sup>O). The most common configuration (i.e., those actually detected by the instrument) are <sup>12</sup>C<sup>16</sup>O<sup>16</sup>O (44), <sup>13</sup>C<sup>16</sup>O<sup>16</sup>O (45), and <sup>12</sup>C<sup>18</sup>O<sup>16</sup>O (46). “Heavier” configurations (e.g., <sup>13</sup>C<sup>18</sup>O<sup>16</sup>O) are very rare, and therefore not significant.

### 3.2 Isotope fractionation

Differences in physicochemical properties (e.g., thermodynamic properties, differences in motion and reaction rates) between isotopic atoms or compounds with the same number of protons and different neutron numbers result in isotopic fractionation during various geochemical interactions in nature. It consists of the “separation” between isotopes of the same element during chemical, physical and biological processes, which ultimately results in a different concentration of each isotopic species in the final product concerning the initial scenario.

Based on the characteristics and reasons, there are two main types of fractionations: *equilibrium isotope fractionation* and *kinetic isotope fractionation*.

*Equilibrium isotope fractionation* means the redistribution of light and heavy isotope atoms or molecules in a system for thermodynamic reasons, resulting in differences in the isotopic composition of each compound or phase. The “thermodynamic reasons” here can be interpreted in two ways: Firstly, the thermodynamic properties of light and heavy isotope atoms or molecules are different (e.g., entropy, enthalpy, internal energy, heat capacity and other thermodynamic parameters); secondly, when the environmental factors (mainly temperature) change, the free energy (ΔE) within a system will also change. Once the ambient temperature is determined and there is no chemical reaction, the system continuously automatically adjusts the distribution ratio of light and heavy isotope atoms or molecules of each compound or phase by means of isotope exchange to reduce the free energy of the system and achieve a stable state of the system. When the ΔE of the system is zero (i.e., when the isotope exchange reaches equilibrium), the isotopic composition of each compound or phase of the system is also determined.

*Kinetic isotope fractionation* is defined as the isotope fractionation caused by minor differences in the physicochemical properties of isotopic atoms or molecules of an element due to differences in their mass numbers, resulting in different rates of reaction or movement during chemical reactions or evaporation. In quantum effects, such differences in reaction efficiency can usually be explained by the fact that, among different isotopes of the same element, the lighter isotope has a weaker

chemical bond than the heavier one and is, therefore, prone to decomposition (Melander, 1960). Kinetic isotope fractionation is accompanied by chemical reactions and phase transitions that occur and are single-phase irreversible processes.

Usually, isotope fractionation provides tiny changes between the source and final reservoirs. Therefore, this difference is given as  $\delta$ , which is the deviation (in ‰) between the isotopic ratio measured in a given sample (x) and that of a standard (std). Take oxygen isotopes as an example:

$$\delta^{18}\text{O}_x = 10^3 * ((^{18}\text{O}/^{16}\text{O})_x / (^{18}\text{O}/^{16}\text{O})_{\text{std}} - 1)$$

Therefore,  $\delta$  is positive if the sample is enriched in “heavy” isotopes; if the sample is enriched in “light” isotopes,  $\delta$  shows negative.

The common reference  $\delta^{13}\text{C}$  marine carbonate standards *PDB* (*Pee Dee Belemnite*) are derived from Cretaceous marine fossils, the *Belemnitella americana* issue found in the Pee Dee Formation of South Carolina, USA. This issue has a higher  $^{13}\text{C}/^{12}\text{C}$  ratio than almost all other natural carbonaceous materials. For convenience, it has been given a value of 0 for  $\delta^{13}\text{C}$ , giving a positive  $\delta$  value to almost all other natural products. This original standard was in use for a long time. However, a new reference was established by a laboratory in Vienna, which gave rise to the widespread use of the “*Vienna Pee Dee Belemnite*”, abbreviated as *VPDB*.

Most isotope analysis results are reported as *SMOW* (*Standard Mean Ocean Water*) for hydrogen and oxygen in the water. It is defined by ANSI (American National Standards Institute) water sample *NBS-1*:  $(\text{D}/\text{H})_{\text{SMOW}} = 1.050$   $(\text{D}/\text{H})_{\text{NBS-1}} = 1.56 \times 10^{-4}$ ;  $(^{18}\text{O}/^{16}\text{O})_{\text{SMOW}} = 1.008$   $(^{18}\text{O}/^{16}\text{O})_{\text{NBS-1}} = 2.005 \times 10^{-3}$ , and its isotopic composition is consistent within the experimental precision range with that determined from average seawater samples from 500 to 2000m depth in the open areas of the Pacific, Atlantic and Indian Oceans. *NBS-1* is distilled water from the Potomac River, USA, with  $\text{D}/\text{H} = 149 \times 10^{-6}$ ;  $^{18}\text{O}/^{16}\text{O} = 1989.4 \times 10^{-6}$ ;  $\delta\text{D} = -47.1\text{‰}$ ;  $\delta^{18}\text{O} = -7.89\text{‰}$  all relative to *SMOW*. Another reference standard distributed by ANSI, *NBS-1A*, is Yellowstone melting snow water with  $\delta\text{D} = -183.2\text{‰}$ ;  $\delta^{18}\text{O} = -24.29\text{‰}$ , also relative to *SMOW*.

### 3.3 Oxygen stable isotope

Oxygen is the eighth element in the periodic table and has the third-highest total mass of any element in the universe, just below hydrogen and helium. Nearly half (46.6%) of the mass within the Earth’s crust is made up of oxygen and oxides. There are 18 known isotopes of oxygen, three of which are stable ( $^{16}\text{O}$ ,  $^{17}\text{O}$  and  $^{18}\text{O}$ ). Of these,  $^{16}\text{O}$ , the light isotope, accounts for the vast majority, with an abundance of 99.76%, while  $^{18}\text{O}$  (the heavy isotope) has only an abundance of 0.20%.  $^{17}\text{O}$  is usually ignored since it is too rare (about 0.04%).

When we talk about stable oxygen isotopes, the first thing that comes to mind is the process linked to the hydrologic cycle since oxygen is the essential component of water (oxygen and hydrogen). The isotopic composition of oxygen in the water cycle changes with processes of evaporation and condensation, which are the main approaches associated with the fractionation of oxygen isotopes, creating a system



of isotopic fractionation (*Rayleigh fractionation*). Therefore, stable oxygen and its isotopes are widely used in paleoceanographic and paleoclimatological research, being important in the paleoclimatic record construction.

Evaporation means the passage from liquid form to vapour form, while condensation is the revert from vapour form to water or crystalline (snow form). As we mentioned above, these processes are involved in fractionation, which leads to an entirely different isotopic composition in terms of source and target reservoir because of the behaviour of isotopic molecules that contain light or heavy isotopes (especially those associated with oxygen rather than hydrogen) are subjected to different behaviour when it comes to thermodynamic reaction. For example, during evaporation, light molecules (molecules that contain  $^{16}\text{O}$ ) are favoured to pass from a liquid form to the vapour form with respect to the heavy molecules, which tend to stay in the liquid state. This allows the final reservoir to be enriched in light isotopes compared to the source reservoir. When it comes to the precipitation (i.e., the condensation process), the molecules with different isotopes have opposite behaviour: water molecules with  $^{18}\text{O}$  have a slightly heavier mass and are more likely to condense and land as droplets or snowflakes; conversely, atmospheric water molecules containing  $^{16}\text{O}$  are lighter in mass and less capable of taking part in this process, tending to remain in the gaseous phase in clouds. As a result, the few heavy isotopic molecules that have passed from the liquid to the vapour form tend to revert immediately into liquid form and return to the source. Suppose we observe condensation, the formation of heavy clouds and the beginning of rainfall. In that case, the first drops will be enriched in heavy isotopes with respect to the later drops. Significant variations in cloud isotopes will occur before and after precipitation (the  $\delta^{18}\text{O}$  values can be from -2‰ to -22‰).

We can see the global hydrologic cycle as a gigantic distillation column, which causes isotope fractionation. The  $\delta^{18}\text{O}$  of source reservoirs (clouds) and precipitation changes in time under the effect of *Rayleigh fractionation*. Precipitation occurs through the movement and cooling of equatorial clouds to higher latitudes or altitudes, during which the  $^{18}\text{O}$  isotope content continues to decrease with time, and the source reservoirs become lighter and lighter. This is referred to as the *rain-out effect*. In this precipitation process, the  $\delta^{18}\text{O}$  is controlled by altitude (*altitude effect*) and latitude (*latitude effect*). Among these, altitude is the most efficient agent, which refers to the  $\delta^{18}\text{O}$  decrease in rainfall with increasing altitude. This effect depends on the local climate and topography. *Latitudinal effects* indicate a gradual decrease in heavy isotopes from low to high latitudes. Surface seawater  $\delta^{18}\text{O}$  reflects local hydrological conditions (e.g., precipitation/evaporation ratio, river runoff). Heavier values correspond to tropical areas with a large amount of evaporation but little precipitation. The surface water here depletes in light oxygen and is rich in heavy oxygen because of the low runoff characteristics. It needs to take a long time to be given back the loss of light isotopes due to evaporation. The equatorial zone, which is located between the tropical zone, has slightly lighter oxygen isotopes compared to the tropical areas since there has still a lot of evaporation while also has a significant amount of rainfall, which leads to

part of the light oxygen immediately rejected into the system by local precipitation. In higher latitudes, a decrease in  $\delta^{18}\text{O}$  related to precipitation here becoming lighter and also having much runoff. Hence the surface ocean is lighter than the middle and low latitudes.

Based on the fact that the atmosphere is a giant “distillator” also, we can observe different compositions in terms of stable isotopes in different areas on the Earth’s surface. Specifically, we know that the precipitation is heavier (i.e., contains more heavy oxygen) in the low latitudes while becoming lighter and lighter as latitude goes towards a high value. Thus, if moving to the poles, we can observe the lightest isotopic composition of the general precipitation.

The composition of ocean water in very low latitudes (near the equator) is considered a standard concentration which means no difference concerning the reference point (i.e., the standard deviation between  $^{16}\text{O}$  and  $^{18}\text{O}$ ). If moved to high latitudes, the composition of precipitation (snow) is in the order of -40‰ to -30‰, which is quite light and rich in light oxygen with respect to heavy oxygen. However, in normal conditions, the ocean is kept in steady-state conditions, meaning there is no significant change in isotopic composition because precipitation is driven back to the ocean by runoff and rainfall. If ice is created in high latitudes, part of the ice will melt later, and the light isotopes trapped in the ice will be conveyed back to the ocean due to the currents and movement within the ocean, transporting the melted water to low latitudes in a short time. This process keeps the ocean in conditions of general equilibrium and happens in relatively short intervals of time because of the mixing of the ocean and the hydrological processes that are involved in this rainfall or snowfall, ice formation and melting usually happen in time intervals in the order of a few thousands of years (commonly 1 to 2 kyr, but in the worst case, may up to 4 kyr). This is linked to the fact that the ocean is an unstable, moving environment. Therefore, we consider the composition of ocean water only slightly diverging from the reference value, which is 0.

However, this is only for today’s situation; the average  $\delta^{18}\text{O}$  values of oceans have changed in geologic time. Until nowadays, there is still very little we know of pre-Cenozoic seas, while better off relying on the “recent” (late Cenozoic) ocean. Past oceans were utterly different in dynamics and compositions from the present day, even in terms of concentration of carbon dioxide and other elements or components. Since it is impossible to estimate the true composition of past oceans, we can consider that the ocean during the last 2 Myr was similar to the present day (i.e., the system’s behaviour is similar). For scientific research which needs to use the isotopic composition of seawater, it is better to stay in the Pleistocene as the lead time we can refer to when we want to discuss the long-term changes in the isotopic composition of the ocean. If beyond this period, during which we may only have a rough idea of the certain ocean composition.

### 3.4 $\delta^{18}\text{O}$ and reconstruction of past climate

One of the main targets for paleoclimate is reconstructing past temperature, which is not based on direct measurement, but the employment of geochemical proxy.

Using stable oxygen isotopes as proxies of temperature and obtaining past climatic conditions are dreams scientists have tried to achieve for many years. People attempt an equivalence (only consider rainfall or snowfall) between temperature changes and the relative changes in  $\delta^{18}\text{O}$  of precipitation by present-day observation of many stations around the world, getting the relationship shows that:

$$1^\circ\text{C} = 0.6 \delta^{18}\text{O}$$
$$\text{Or } \delta^{18}\text{O} (1\text{‰}) \approx 1.7^\circ\text{C}$$

This means that different temperatures from one place to another correspond to a difference in the  $\delta^{18}\text{O}$  of local meteorological composition. However, this relationship only estimates a variation in temperature, ignoring the offset value, which depends on the  $\delta^{18}\text{O}$  source in the geologic past. To reconstruct the past temperature, we also need absolute values. It follows that the questions for scientists:

1. what proxy to use for measuring  $\delta^{18}\text{O}$  in the geologic time;

For example, different species of fossils or rocks.

2. what is the fractionation factor of such a proxy;

Here the researcher needs to explore and ensure the behaviour in terms of fractionation for the used proxy was constant in time and evaluated precisely.

3. how to detect and discriminate any possible diagenetic fractionation.

For instance, if we consider using rocks as a proxy, the process of transformation from mud to rock also implies changes in the chemistry, which provides the variation in the isotopic composition.

Harold Urey (Urey, 1948) provided pioneering ideas for solving some of these problems. As a geochemist, Urey was obsessed with the idea of measuring and reconstructing the temperature during the geologic history of the Earth and was the first one to guess and understand that the  $^{16}\text{O}/^{18}\text{O}$  ratio in shell calcite is controlled by the environmental temperature of the seawater. In 1948, he demonstrated that the equilibrium isotope fractionation between  $\text{H}_2\text{O}$  and  $\text{CaCO}_3$ , the main component of fossils and sedimentary rocks, mainly depends on temperature by means of making live observations on present shells. Hence, the  $^{16}\text{O}/^{18}\text{O}$  ratio in biogenic calcite reflects the water temperature where the mineral precipitated. This is the beginning of using the  $\delta^{18}\text{O}$  of fossil carbonates as a paleothermometer. Urey built a simple model carried out in a fish tank by setting specific environmental conditions to control the isotopic composition of the shell (the organisms used here were bivalves, i.e., the proxy Urey chose) to retrieve and get the temperatures at which bivalves grew. From this experiment, Urey employed  $\delta^{18}\text{O}$  to construct the relationships between water temperature and  $\delta^{18}\text{O}$  of organism calcite. Essential conclusions were thus observed: all shells independent from temperature are characterized by a isotopic composition heavier than the ambient water. And still, the relative enrichment of  $^{18}\text{O}$  that depends on the fractionation factor decreases as temperature increases. This enrichment is evident depending on the temperature at which animals live.

Based on the observation that was made by Urey, Epstein (Epstein *et.al.*, 1951) and some other scientists published the first equation for calculating paleotemperature

in 1951:

$$T = 16.5 - 4.3 (\delta_{\text{card}} - \delta_{\text{sw}}) + 0.14 (\delta_{\text{card}} - \delta_{\text{sw}})^2$$

Where:

T = water temperature

$\delta_{\text{sw}} = \delta^{18}\text{O}$  of water at T

$\delta_{\text{card}} = \delta^{18}\text{O}$  of  $\text{CaCO}_3$  (measured)

If the equation is shown on the axes, it will be a parabolic trend, which has offset to shift the curve depending on different  $\delta_{\text{sw}}$  values. To give a solution to this approach, authors took for granted that  $\delta_{\text{sw}}$  was constant in time. This certainly seems problematic today, but the equation achieved an important demonstration that carbonates with “heavier” isotopic composition were precipitated in colder waters. This was also the basis for previous model development and the expectations of scientists at that time.

From the 50s beginning to the end of the 80s, Epstein’s equation was amended and adapted by a lot of different scientists, some variations are shown below.

For bivalve shells calcite:

$$T = 17.04 - 4.34 (\delta_{\text{card}} - \delta_{\text{sw}}) + (\delta_{\text{card}} - \delta_{\text{sw}})^2 \text{ (Epstein } et.al., 1953)$$

$$T = (\delta_{\text{card}} - \delta_{\text{sw}}) + 28.8 / 2.67 \text{ (Oba and Horibe, 1972)}$$

For gastropods aragonite:

$$T = 21.8 - 4.69 (\delta_{\text{aragonite}} - \delta_{\text{sw}}) \text{ (Grossman and Ku, 1986)}$$

Urey soon realized that bivalves were not adequate fossils as a proxy to measure and construct paleotemperature even if it is easy to pick with large shells, because it is difficult to find the continuous record of bivalves in the geologic time, especially for some given interval of time, and bivalves’ distribution is also restricted to sedimentary facies. However, almost in the same period (the 60s to the 70s), the exploration of ocean floors began, also known as DSDP (Deep Sea Drilling Project), a lot of cruises that provided vast amounts of sediment cores which contained extensive amounts of planktic foraminifers in most cases and also a few benthic foraminifers in same samples. Compared with bivalves, planktic foraminifera are abundant in the stratigraphic record since the end of the Jurassic and have virtually ubiquitous distribution as they live in the water column and can also be transported to the shore or open ocean; thus, it is no need to consider the sedimentary facies here like bivalves. Most importantly, foraminifera are usually in equilibrium with the environmental seawater during isotopic fractionation, while bivalves, in many instances, secret their shells not in equilibrium with the water so that there is no direct response between the composition of shells and the former water composition; researchers may suffer from different offsets. (This part is described in more detail later in the Foraminifera section.)

With such differences and the advantages of planktonic foraminifera in the study of past temperatures, Urey decided to move from bivalves to planktic foraminifera as a new paleothermometer. To deal with these new, untouched sediment cores, Urey commenced investigating planktic  $\delta^{18}\text{O}$  with the help of a young Italian fellow, Cesare Emiliani. Emiliani collected different species of planktic foraminifera from sediment cores and made an analysis of their tests. By using the  $\delta_{\text{card}}$  values obtained

from the measurements and the formula  $T = 17 - 4.5(\delta_{\text{card}} - \delta_{\text{sw}}) + 0.03(\delta_{\text{card}} - \delta_{\text{sw}})^2$ , Emiliani obtained curves of estimated temperature versus core depth (corresponding to age from new to old) and eventually published the first records reconstructed for the late Quaternary from Piston Core A-1749 in Caribbeans. This kind of data had never been seen before at that published time; the whole scientific community concerned was almost in a state of shock because of it.

Different curves from the records Emiliani built can indicate particular responses of the species in different climatic conditions. However, the offset between different species is virtually constant for main changes in time, making the curves similar in shape. Therefore, the trends are virtually recognizable everywhere independently from the species. One point to note is that,  $\delta_{\text{sw}}$  was still considered to remain constant during the whole period for all the investigated species in this case. Emiliani and Urey knew this problem, but the only way they could do at that time was to simply tweak the value of  $\delta_{\text{sw}}$  in the equation base on the knowledge they knew about the study setting (e.g., surface water temperature) to account for the geographical position of the sediment cores was collected. This does not completely account for the natural variability we observed in the past because they only corrected for the modern values but ignored the past value.

There were two parameters that needed fixing during reconstruction temperature in this case:

1. Latitude where the cores were collected;

The isotopic composition of surface seawater is different in terms of latitudes due to the fractionation of isotopes during the water cycle and river runoff, as described above. In general, heavier  $\delta^{18}\text{O}$  values for surface ocean correspond to the tropical zone where evaporation processes are more frequent than precipitation processes; the equatorial zone with more precipitation happened has slightly lighter values than the tropics, while a decrease in  $\delta^{18}\text{O}$  can be found in high latitudes related to the fact that precipitation becomes lighter here and also has a certain amount of runoff. Based on this basic oceanographic information, Emiliani and Urey estimated the situation on Caribbeans, corrected  $\delta_{\text{sw}}$  used to solve part of the problem.

2. Glacial dynamics.

Glacial dynamics is a simple mechanism based on the isotopic study: during a glacial period, the ocean is enriched in  $^{18}\text{O}$  since precipitation  $^{16}\text{O}$  is stored in ice caps. Therefore, in an interglacial condition like today, the ice caps are not growing in the global amount (i.e., melting rather than growing); continental ice, which is very light in isotopic composition, melts a lot of  $^{16}\text{O}$  to go back to the ocean, keeping the ocean in the state of equilibrium. In this case, we may consider the ocean to be at the reference level because the loss by evaporation is given back to the ocean by precipitation and runoff. However, when the climatic condition changes into an ice age, the extent of the ice cap increases, a large amount of light oxygen was lost by the ocean, providing the precipitation will be restored away to the polar region, the ocean will change its composition and become increasingly heavy in mid to long term. Urey and Emiliani were aware of this phenomenon, but

they could not estimate the extent of it; they considered that this effect is certainly existing, but it is not effective when it comes to the calculation of past temperature since the composition of the ocean remains relatively the same in the long term. That is an underestimation and the biggest mistake in this research from the results of subsequent studies.

After that, Urey and Emiliani published another craze for the scientific community. They measured  $\delta^{18}\text{O}$  records using planktonic foraminifera in sediment cores at different locations worldwide, obtaining curves of  $\delta^{18}\text{O}$  values with different core depths. With the help of the Chronos tag's correspondence, each of these records is linked to the other, and curves retrieved from different locations (respectively, located in the southern Atlantic, Caribbean and the southern Indian Ocean) more or less reflect the same history. Moreover,  $\delta^{18}\text{O}$  curves oscillate cyclically, and the contrast between "light" Holocene values (i.e., modern value) and the "heavy" LGM (Last Glacial Maximum) values may reach 2%, here they are also referred to as the warmest and coldest interval in the last 1 kyr. With these observations, Urey and Emiliani made the significant and influential conclusion that curves are perfectly correlative, even if they were collected in distant locations; thus, these curves probably reflect some global extent.

Since the publication of this vital result that  $\delta^{18}\text{O}$  curves reflect globally the climate cyclicity documented locally, many relevant studies have investigated for decades. In spite of the general enthusiasm for the new method, many remained sceptical about the reliability of  $\delta^{18}\text{O}$  as a paleothermometer. We can conclude that  $\delta^{18}\text{O}$  is an approach that allows us to quantify because it has a punctual description of climatic changes that were also documented in continental records. Nevertheless, the question of whether it is possible to obtain past temperatures with  $\delta^{18}\text{O}$ , as developed here, still requires research and discussion. For Urey and Emiliani, the answer to this question was yes. However, some parts were not working properly in their construction: Epstein's equation involves two variables, namely  $\delta_{\text{card}}$  and  $\delta_{\text{sw}}$ ;  $\delta_{\text{card}}$  was measured in the experiment, while the certain value of  $\delta_{\text{sw}}$  was skipped by considering that  $\delta_{\text{sw}}$  has hardly changed in time and simply corrected by the value of latitude since nobody had a clue on how to measure  $\delta_{\text{sw}}$  in the geological past, Urey and Emiliani's opinion is considered to be over-optimistic. Also, if an assumption is made for the formula used (i.e.,  $T = 17 - 4.5 (\delta_{\text{card}} - \delta_{\text{sw}}) + 0.3 (\delta_{\text{card}} - \delta_{\text{sw}})^2$ ) that its  $\delta_{\text{sw}}$  value is 0 (or any other value, since a change in this value does not affect the relationship between the maximum and minimum values of T, but only changes the absolute value of the offset), corresponding to  $\delta_{\text{card}}$  value with a potential shift of about two from the LGM to modern day (from 0.5‰ to -1.5‰) at the Equator, we can obtain that there will be a 9°C (from around 15°C to 24°C) offset happened during this period. Once the "gap" of temperature in the same interval is transferred to mid-latitude, estimation in the contrast between LGM and modern time increases to 30°C, and this figure even can reach 70°C at the pole. This is an unlikely phenomenon, therefore, it can be concluded that it is unrealistic that  $\delta_{\text{card}}$  varied in time only because of temperature. The value of temperature obtained by simply applying the formula of Epstein to planktic foraminifera is unreliable,

and there is also the glacial effect (as noted above) involved in the construction of  $\delta_{\text{card}}$  apart from the temperature. The  $\delta_{\text{card}}$  in the ocean increases due to both decreasing temperature and the waxing of continental ice caps. New questions have arisen for the reconstruction of past temperatures: how to discriminate glacial effect and temperature in the  $\delta^{18}\text{O}$  of planktic foraminifera?

In this phase of the scientific crisis, Nick Shackleton, another pioneer and genius of paleoceanography, entered the scene. Shackleton (Shackleton, 1967) reckoned the glacial effect as the main “engine” of the oscillation documented in  $\delta^{18}\text{O}$  records. To demonstrate so, he followed a simple but brilliant way of investigating benthic foraminifera instead of planktic foraminifera and completely changed the whole direction of paleoclimatic research. Benthic foraminifera (There is a more detailed description in the subsequent section, “Benthic foraminifera”) live in or on the sediments on the sea floor, where has temperature in the order of about  $2^{\circ}\text{C}$  nowadays; when the situation moves towards ice ages like LGM, the temperature at the seafloor is also around  $1^{\circ}\text{C}$  similarly, as the sea will completely freeze if it falls below  $0^{\circ}\text{C}$  (obviously, this is not possible). Thus, living in a buffered environment, at which ambient temperature can be considered to remain stable in time, benthic foraminifera attracted the attention of Shackleton. Shackleton chose to reverse the approach, which is looking for temperature based on  $\delta_{\text{card}}$  and  $\delta_{\text{sw}}$ , using the known temperature (around  $0^{\circ}\text{C}$ ) and measured  $\delta_{\text{card}}$  to calculate  $\delta_{\text{sw}}$ . Also, another strategy proposed by him, Shackleton advised using the records which were recovered in high latitudes instead of other places. Similarly, the temperatures are virtually the same at the sea bottom anywhere on the Earth, independent of the ocean surface temperature. However, in the high latitudes where surface water is equivalent to cold in an interglacial or glacial condition, the temperature of the sea bottom is similar to the ocean surface. Even if we work on planktic foraminifera in high latitudes, the species used are adapted to cold waters, and we can consider the surface temperature in these regions to be constant in time. The approach of Shackleton aims to choose some settings where the temperature remains constant virtually in time to eliminate the effects of temperature variations.

With such highly innovative theories, in subsequent studies, scientists found that the shape of the  $\delta^{18}\text{O}$  curve with core depths about the benthic foraminifera was similar to the shape of curves that were generated by the study of planktic foraminifera, e.g., the study in Core V22-108, Antarctic Ocean (Charles and Fairbanks, 1990). What is more, based on this approach, it also was possible to estimate that the glacial effect is not negligible as Urey and Emiliani proposed, but this effect may account for around 65% to 95% of benthic foraminifera by comparing the benthic  $\delta^{18}\text{O}$  (formed at constant and low temperature) and the planktonic records which were formed where temperature changes significantly. This discovery was undoubtedly a revolution in the study of  $\delta^{18}\text{O}$  isotope science. Shackleton (Shackleton, 1987) also provided further input to the scientific community: if researchers have estimated the capacity of the glacial effect to provide changes on the isotopic signal of foraminifera, they may also try to estimate the glacioeustatic effect (i.e., attempting to measure the amount of ice formed

during the glacial period). The idea from Shackleton was that measuring benthic  $\delta^{18}\text{O}$  is possible to “weight” continental ice caps, and that can be obtained by means of a simple mass balance, which also permits evaluating the glacioeustatic effect. With a simplified hypothesis, all the water seized from the ocean is turned into ice (i.e., not considering the amount of water vapour recycled as rainfall; this simplification is rather credible regarding the reliabilities of the results; and also validated by independent approaches.) and the information on the composition of water and carbonates, it is possible to estimate the extent of ice glaciers. Ice caps grow as the climate cools, and the oceans provide the amount of sealed ice that increases on the continent; thus, we can expect the global sea level to decrease to account for the fact that most of the water is stored, generated by evaporation from the ocean and stored on the continental ice. To be more specific, the global  $\delta^{18}\text{O}$  is the sum of fractionations within each individual reservoir which has a specific  $\delta^{18}\text{O}$  and capacity of water. At the same time, the total amount of stable isotopes remains the same (simply moving from one reservoir to the other and continuing recycling). For instance, during the ice age, the ocean reservoir becomes smaller in capacity, and its  $\delta^{18}\text{O}$  value changes, whereas the contrast is in the case of continental ice. In a closed system with only two components: ocean and continental ice, we can simplify by applying the concept of relative abundance F (with  $F_w + F_g = 1$ ):

$$\delta^{18}\text{O}_{\text{tot}} = \delta^{18}\text{O}_w F_w + \delta^{18}\text{O}_g F_g$$

where  $F_w$  is the capacity of water,

$F_g$  is the capacity of ice;

$\delta^{18}\text{O}_w$  is the  $\delta^{18}\text{O}$  of water,

$\delta^{18}\text{O}_g$  is the  $\delta^{18}\text{O}$  of ice and

$\delta^{18}\text{O}_{\text{tot}}$  is the total amount of  $\delta^{18}\text{O}$ .

since  $F_w + F_g = 1$ ,

$$\delta^{18}\text{O}_{\text{tot}} = \delta^{18}\text{O}_w F_w + \delta^{18}\text{O}_g (1 - F_w).$$

For the mass conservation principle,  $\delta^{18}\text{O}_{\text{tot}} = 0$ . The known ice  $\delta^{18}\text{O}$  in the polar area is -40‰, and ocean  $\delta^{18}\text{O}$  during the LGM was 1.65‰, hence:  $F_w = 96\%$ ;  $F_g = 4\%$ . The calculated relative abundance of water and ice during LGM is reasonable with the estimates of the total extent of glaciers: since the LGM, the ocean basin shape did not change, and glacioeustatism accounts for 4% of *Mean Ocean Depth*, the decreased mean sea level depth may be around 150m; this datum is confirmed by marine terraces observations.

However, back to the question of whether it is possible to obtain past temperatures with  $\delta^{18}\text{O}$  and how to translate  $\delta^{18}\text{O}$  into temperature; like the previous description,  $0.6\text{‰} (\delta^{18}\text{O}) \approx 1^\circ\text{C}$  in meteoric water, what happens in the oceans? Even though we know the expansion of ice caps follows a decrease in global temperature, the calculation is still complex because all the available proxies have issues. Urey’s equations work with calcite shells precipitated in equilibrium with seawater, while many marine calcite producers (e.g., coccoliths, echinoids, molluscs) do not respect the rule. The most reliable proxies are foraminiferal species (both planktic and benthic) with constant offsets, which allows for simple corrections. However, this also becomes much more complicated by the fact that foraminifera is known to



reflect mostly the glacioeustatic phenomenon rather than temperature. In the subsequent studies, based on the analysis of specific species of foraminifera (orbulina universa) that were grown in fish tanks under controlled conditions, available data suggest that, for planktic species in ideal conditions,

$$1 \text{ ‰ } (\delta^{18}\text{O}) \approx 4 \text{ }^\circ\text{C}$$

This relationship is rough as it is only demonstrated under specific controlled conditions. By simulating changes in environmental conditions (e.g., light or nutrients) during the experiment, researchers found that the environmental conditions can even overtake the main signal temperature and complicate calculations. To date, no more effective method has been proposed to reconstruct past ocean temperatures using  $\delta^{18}\text{O}$ .

$\delta^{18}\text{O}$  can also be employed by other organisms (i.e., corals, belemnites, diatoms, and conodonts); although there have been many data studies currently, it is still hard to understand how these animals utilized oxygen in the past. Also, in addition to the different cruise programs which collected ocean sediments as the main source of the proxy from the 60s onwards, such as DSDP (Deep Sea Drilling Project), ODP (Ocean Drilling Program) and IODP (Integrated Ocean Drilling Program; International Ocean Discovery Program), many ice cores have been drilled in different projects since 70s, with different length records, like GISP (G. Ice Sheet Project), GRIR (GR. Icecore Project), VOSTOK, RU-F-USA and EPICA (EU Proj. Ice Coring Antarct). In these archives, ice and ocean sediments can both recover  $\delta^{18}\text{O}$ . In contrast, their curves are the opposite, as the transportation and fractionation of isotopes during the different processes.

The stable oxygen isotope records can provide an effective long-distance correlation tool. A common language is required to make stratigraphy with  $\delta^{18}\text{O}$  records. Hence MIS (*Marine Isotope Stage*) and OIS (*Oxygen Isotope Stratigraphy*) were marked and widely used: MIS is the oxygen isotope records including major glacial and interglacial periods and fewer oscillations and events. As we said above, it is employed globally as a useful correlated tool and published by Emiliani; and OIS is the subdivision of isotopic records based on the recognition of peculiar signatures and pattern. Stratigraphy made on isotopic record is usually know as OIS, researchers can subdivide their records into interval by characterized light and heavy isotopic conditions to obtain a succession of subdivision events and their own OIS.

MIS are numbered backwards with increasing values beginning from the present interglacial (i.e., MIS1); even numbers correspond to glacial condition, and odd ones refer to interglacial condition. Lesser oscillations within the major period, if documented globally, are also labelled (e.g., MIS15.3, MIS15.2 and MIS15.1). The boundaries of MIS are located at midpoints of glacial to interglacial transits and vice-versa.

We know that correlations can be made on long distances; for example,  $\delta^{18}\text{O}$  records from the Atlantic Ocean correspond well to the Pacific Ocean since they both primarily respond to glacioeustatic forcing. However, the situation in the Mediterranean Seas has some particular. As described earlier, the Mediterranean is

a basin of intense evaporation processes, with particular climatic conditions and high salinity and temperature characteristics. Therefore, the records from the Mediterranean Seas represent both the glacioeustatic forcing and local climatic conditions, showing different fluctuations within the major intervals.

Nowadays, scientists tend to rely less on single individual isotopic records, which are easily affected by local problems: being controlled to varying degrees by temperature, salinity and nutrition, changing the precipitated calcite composition. A more common research approach is “isotopic stacks”, which means overlapping many records together and filtering the disturbing signal to clean the record’s local peculiar (e.g., LP04<sub>benthic</sub> curve, which is made of 55 different separated records).

### 3.5 Carbon stable isotopes

Carbon is a non-metallic element with the chemical symbol C. It is stable at room temperature, non-reactive, and has very low toxicity to humans. As an ubiquitous element, Carbon is widely present in the atmosphere, the Earth’s crust and living things in many forms.

There are fifteen carbon isotopes known, ranging from  $^8\text{C}$  to  $^{22}\text{C}$ , of which  $^{12}\text{C}$  and  $^{13}\text{C}$  are stable and the rest are radioactive, with  $^{14}\text{C}$  having a half-life of 5,730 years and the others being unstable. In the Earth’s natural environment,  $^{12}\text{C}$  accounts for 98.93% of all carbon, while  $^{13}\text{C}$  accounts for 1.07%.

C forms compounds (both organic and inorganic) that are preserved in separate reservoirs, which continuously exchange matter from one to the other. Any carbon transport between different reservoirs induces isotopic fractionation; since there are continuous flows between different reservoirs, the isotopic fractionation happens strongly and the isotopic signature of these transformation change from one status to another. Most of these changes are made of the  $\text{CO}_2$  transfer, as  $\text{CO}_2$  is a resilient molecule and easy to move with respect to the solid state of carbon (e.g., diamond which is made of pure carbon and challenging to be employed and transported into other reservoirs.), for example, it can be employed by plants to make photosynthesis and used by rocks to change the chemistry features.

According to the wide distribution of carbon, people commonly define several essential reservoirs in the natural system. Furthermore, the amount of C is indicated as Gt (gigatons, also known as billions of tons). The smaller reservoirs are provided by life (both vegetation and animal), giving an amount of 700Gt, which is minimal quality concerning other reservoirs, e.g., deep ocean or sediments and rocks have masses of 38,000Gt and 66,000,000Gt respectively. The atmosphere contains almost the same amount of carbon stored in vegetation, about 600Gt; it should be mentioned here that this value is referred to pre-industrial conditions, as the number of industrial activities has increased, the value increases accordingly. These two reservoirs described above are located in the superficial part of the planet with the most active dynamics. Hence they are not capable of storing large amounts of carbon. The opposite situation is the “hidden” reservoir which stores an enormous amount of carbon in the deep ocean, sediments and rocks (there is a distinction between sediments and rocks, sediments are intended as loose and uncompacted

status while rocks are solid and crystalline form which is even more effective in retaining carbon compare to loosen sediments.) or coal and crude oil. As coal and crude oils can represent huge reservoirs, the problem of exploiting hydrocarbons for fuel linked by human activities becomes progressively worse based on the fact that these huge reservoirs are resurfaced and free a lot of carbon that was stored and intended to stay for millions year, immediately into the atmosphere.

The “hidden” reservoir represents by clathrates, which are conglomerates of water ice crystals, linked by H bonds, trapping gas molecules of hydrocarbons. Usually, they are light organic carbons, predominantly methane, also ethane and propane, forming in conditions of high pressure and low temperature (e.g., into loose sediments on the ocean floor). Thus, clathrates are often found at the base of continental scarp, where temperatures at about 0°C and the load of the water column provides the pressure. Generally, these reservoirs have been found so far are located close to continental margins, with an incredible amount of methane which is used as fuels for burning. Since methane is a greenhouse gas, the “hidden” reservoirs have a potential environmental risk; the destabilization of clathrate due to changes in pressure and temperature conditions may lead to climate crises by the immediate release of methane into the ocean and the atmosphere. Such a situation occurs once the sea level drops (with a concomitant drop in temperature), with a corresponding pressure drop. The  $\delta^{13}\text{C}$  of  $\text{CH}_4$  in clathrates is extremely light (less than -60‰, decreasing in the gaseous phase), producing distinctive isotopic signatures of clathrates and possibly documented in the geologic record.

Each of these reservoirs is capable of storing carbon in different forms. Carbon dioxide is the main component made of carbon in the atmosphere, while carbon is stored as organic tissue mainly in vegetation, animals and soils. Since soils are mainly made of vegetation debris, there are both decomposed vegetable tissues and vegetal tissues in soils. By fermentation of the vegetal tissues,  $\text{CO}_2$  is generated and can be free into the atmosphere or retained in the soils. Thus, the coexistence of inorganic compounds, organic compounds and  $\text{CO}_2$  happened in soil reservoirs which are attributed as effective storage since containing the double amount of carbon with respect to life. In the deep ocean, most carbon here is represented by  $\text{CO}_2$  but also has organic matter debris (both vegetal and animal debris). Sediment and rocks, especially carbonate rocks, contain carbon as a crystal component.

At any time, the transformation of carbon from one reservoir to another will change the isotopic composition of reservoirs. There are different ranges in  $\delta^{13}\text{C}$  depending on the reservoirs. The ranges can be characterized by broad or narrow, that is  $\delta^{13}\text{C}$  of variation in the same reservoir; for example, the  $\delta^{13}\text{C}$  of atmospheric  $\text{CH}_4$  varies only within a small range at about -48‰; oceanic dissolved inorganic carbon (DIC) also has a narrow range around 0‰ which is the reference of the isotopic analysis, i.e., standard mean ocean water (SMOW). Virtually, most the reservoirs are presented with negative values, in addition to metamorphic  $\text{CO}_2$ , groundwater DIC, marine limestone and DIC. The most positive values may counterpart metamorphic  $\text{CO}_2$ , which is less than 10‰, while the negative values can reach values as low as -80‰, which is incredibly light with respect to the most positive one. Researchers

can approximate the reservoir source of the substance from the  $\delta^{13}\text{C}$  value.

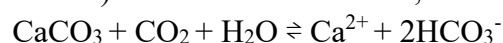
Reservoirs continuously exchange carbon with each other at different time scales. The most rapid flux occurs in the upper part of the Earth (both in the ocean and continent). These shallow carbon exchanges (atmosphere, biosphere and shallow ocean) mainly occur by  $\text{CO}_2$  with the highest velocity (months or years). Vegetation can effectively exchange carbon with the atmosphere and soils (e.g., leaves fall to the ground and become part of the soil). Therefore, carbon can be stored by photosynthesis as organic matter in the plants and transferred to the soils in terms of vegetable debris which can degrade to provide a source of  $\text{CO}_2$ . The amount of carbon released from the atmosphere to the ocean is almost equal to the amount received from the upper ocean, with the atmosphere possibly absorbing slightly more. The fast exchange could be related to the fact that these reservoirs are small and incapable of retaining carbon.

The other side is the deeper part of the planet; fluxes become much slower due to the thermocline, in the order of centuries or thousands of years; they respond to the oceanic circulation patterns. There is also sedimentation which is faster than the movement of water mass; however, when considered in terms of the global ocean, and not just basins with high sedimentation rates, most exchanges are related to the movement of water mass from the upper domains to the deep domains, and vice versa.

The fluxes between sediments and the rest of the dynamic part of the Earth (i.e., the atmosphere and the ocean) are usually extremely slow, such as black shales made of coal, preserving organic carbon for hundreds of million years. It takes a lot of time for sediments to fall and transport into rocks; in the meantime, these rocks can be attacked by chemical reactions to be dissolved and destroyed, finally, recycled back into the atmosphere or directly into the ocean.

The deep Earth generates  $\text{CO}_2$  with variable rates (for today, about 2Gt per year). As the exchange cannot be controlled in a given time scale, occasional releasing of  $\text{CO}_2$  and consumption of  $\text{CO}_2$  contributed to the “erratic” fluxes. The typical example of this process is associated with volcanic activity, in which eruptions happen randomly and can be significant in terms of releasing  $\text{CO}_2$  with respect to other activities (e.g., offspring). Although such input of  $\text{CO}_2$  into the atmosphere occurs by chance, it is crucial for the content of the atmosphere and the Earth today; according to models of the Earth’s evolution, there would be no  $\text{CO}_2$  in the atmosphere without volcanic activity, which means without the chance to provide enough  $\text{CO}_2$  to sustain the Earth system, especially to sustain the minimum amount of  $\text{CO}_2$  which is required by plants to survive.

$\text{CO}_2$  is involved in the surface alteration processes of rocks, both carbonate (by dissolution) and silicate (by hydrolysis). Such processes allow for a seizing of atmospheric carbon on a geologically significant time scale. Depending on whether it is a carbonate or a silicate rock that is reacting, different processes can take place: dissolution (karstification) affects carbonate rocks,

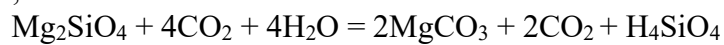


Carbonate rocks need carbon dioxide and water to conduct reversible chemical

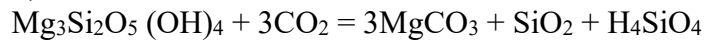
reactions; precipitation may occur once the carbonate rocks are dissolved. As reversible reactions do not allow for a long-term (i.e., geologically significant) seizing of CO<sub>2</sub>, karstification is a zero-balance process.

Hydrolysis affects silicate rocks with a wide range of processes that may occur in silicate rocks; it controls the concentration of CO<sub>2</sub> in the atmosphere by the *silicate pump*, which is in turn regulated by temperature, pressure and vegetation cover (which also responds to the concentration of atmospheric CO<sub>2</sub>). With a warmer climate, temperature, precipitation and vegetation increase accordingly, leading to enhanced chemical weathering, which removes the CO<sub>2</sub>; in the long term, the initial warming reduces with the decrease of greenhouse gas. On the contrary, when the climate cools, temperature, precipitation and vegetation cover are subsequently reduced, and less weathering and dissolution of silicate rocks happen, resulting in reduced absorption and utilization of CO<sub>2</sub> and buffering the decrease in temperature. The following is the process of hydrolysis of some silicate rocks:

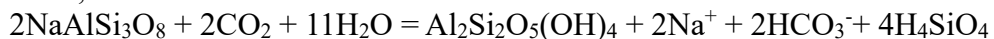
for forsterite,



for serpentine,

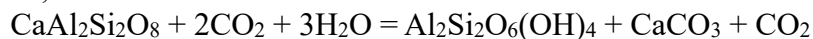


for albite,



The point to note is natrite (i.e., Na<sub>2</sub>(HCO<sub>3</sub>)<sup>2</sup>) here only precipitates in super-arid areas (e.g., deserts).

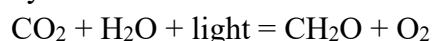
for anorthite,



These processes can be more effective in solvent rock than karstification and become active when there are warm climatic conditions, while also include some tectonic effects such as uplifting mountains (made of silicate rocks): CO<sub>2</sub> would be involved in consuming the new silicate rocks and the excess of consumption potentially provide a significant drop in temperature which is unexpected by the climate system. For example, during the Pleistocene, two massive glaciations are relatively equivalent to two significant orogeny events, Caledonian and Variscan.

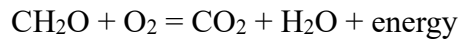
Carbon stable isotopes and oxygen stable isotopes are often obtained simultaneously when researchers analyse isotopic compositions, such as shells. The study of carbon isotope is basically based on the investigation of the relationship between the heavy isotope (i.e., <sup>13</sup>C) with respect to the concentration of the light isotope (i.e., <sup>12</sup>C), potentially important for paleoclimatic and paleoenvironmental studies. However, compared to the oxygen isotopes, the interpretation of carbon signal is very complex, composed of a lot of information that's mingled together and difficult to discriminate. This is related to the fact that carbon is involved in more processes than oxygen, and part of the reactions involved are biological and others are inorganic. Carbon is not only involved in the hydrological cycle as CO<sub>2</sub> is part of the atmosphere and also in the geochemical and biological cycle (namely the biogeochemical carbon cycle).

C is an essential element for plants' and animals' life. CO<sub>2</sub> is employed by plants in order to make photosynthesis:



The CH<sub>2</sub>O here is the simplification of C<sub>6</sub>H<sub>12</sub>O<sub>6</sub>, which represent organic matter, basically glucose or sugar.

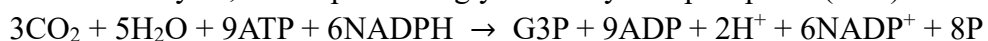
Oxygen is a powerful oxidizer that may degrade plants if not exhausted in time. During the night, in the absence of light, plants consume oxygen through the respiration process:



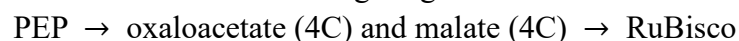
Organic matter was burning with oxygen to produce CO<sub>2</sub>. Both equations above occur at equilibrium and are thus associated with a strong fractionation in carbon isotopes. The composition of CO<sub>2</sub>, as a product of respiration, is different from the organic matter that process happened before in terms of isotopic point of view. Thus, a further step in the process leads to conclude that the isotopic composition between the atmosphere and the plant tissues is very different.

Plants prefer to use CO<sub>2</sub> containing light carbon isotopes (<sup>12</sup>C) as the bonds that involve light isotopes are weaker than the heavy ones, and it is simpler to break the bonds linked to light carbon. Also, fractionation differs between algae and terrestrial plants, and also amidst the latter. Three photosynthetic mechanisms exist (C<sub>3</sub>, C<sub>4</sub> and CAM) that characterize plants that live in different climatic conditions with different ecology and provide unique degrees of fractionation:

1. C<sub>3</sub> plants live in temperate climates and favourable settings which mean no risk of drying up, use the Calvin-Benson photosynthetic pathway. Their stomata are large and easily remain open, allowing for a continuous and intense flux from the atmosphere to the inner part of the leaf. CO<sub>2</sub> is attached to a substrate which is an enzyme called RuBisCo; by employing energy, RuBisCo and CO<sub>2</sub> are transformed into G3P, an omnipotent molecule. C<sub>3</sub> plants can afford to discriminate CO<sub>2</sub> molecules and fractionate vigorously. This strategy is employed by 97% of the known plants nowadays and involves the use of atmospheric CO<sub>2</sub>, which is immediately transferred into the metabolic cycle of plants. C<sub>3</sub> plants only use the Calvin-Benson cycle, which produces glyceraldehyde 3-phosphate (G3P):



2. C<sub>4</sub> plants thrive in harsh environments and use the Hatch-Slack pathway. In this case, there is a “barrier” (mesophyll cell) that protects the cells that make photosynthesis, and stomata are scarce and small, kept extremely close, leading to reduced gaseous exchange, and CO<sub>2</sub> intake is weak. All the molecules that represent the substrate of CO<sub>2</sub> are contained four atoms of carbon (the origin of the plant’s name); after CO<sub>2</sub> is transported to the Bundle Sheath cell where the Calvin cycle happens, the number of carbon atoms contained in the molecule changes to three, and the reaction of C<sub>3</sub> plants occurs. The C<sub>4</sub> and C<sub>3</sub> reactions are spatially separated. They cope with low concentrations of CO<sub>2</sub>, high light, high temperature, drought, and high salinity. C<sub>4</sub> plants cannot discriminate CO<sub>2</sub> molecules as they could; thus, fractionation is reduced. Most of C<sub>4</sub> plants are grasses (e.g., corn, sugarcane and sorghum). Active transfer of CO<sub>2</sub> through organic acids:



3. CAM plants (less than 1% of the known plants develop this strategy), e.g., Cactaceae, living in desert areas, employ the Crassulacean acid metabolism. Their

stomata open only at night and under the rain ( $C_4$  cycle occurs) to allow for the intake of  $CO_2$  and then keep close during the day. The  $C_3$  cycle is carried out in the sunshine; therefore, the  $C_3$  and  $C_4$  reactions are temporally separated and this mechanism has the weakest fractionation.

Due to differences in the strength of isotopic fractionation, even if the isotopic composition of atmospheric  $CO_2$  sources is the same,  $C_3$  and  $C_4$  plants are known to have different isotopic ranges, with  $\delta^{13}C$  values around -25‰ and -13‰, respectively.

In the continent, vegetation works as biological pumps. For example, in a mature forest, the seizing of  $CO_2$  from the atmosphere forms organic matter (happens in leaves), and the same organic matter is also released to the ground when the leaves fall, or plants die. In this case, the oxidation of the organic matter happens and releases  $CO_2$  into the atmosphere later. Therefore, the mature forest does not seize  $CO_2$ ; the amount of  $CO_2$  employed is the same as that released and has the opposite condition to the growing forest, which seizes  $CO_2$  effectively.

Carbon is a resilient signature in organic matter, and we can employ its peculiar isotopic composition of carbon that characterize the organic matter as a tracer to detect sources. E.g.,  $C_3$  and  $C_4$  plants have distinctive values; alcohol may add sugar to increase the alcoholic degree, and carbon can be used here to detect where the alcohol is derived. Different animals have different “recipes” depending on their habits; hence carbon signal is pervasive also into animals. For instance, grizzlies and black bears have different  $\delta^{13}C$  based on the fact that black bears feed on plants (e.g., nuts and berries) which are very light in isotopic composition, while grizzlies also eat fishers (e.g., marine salmon), have heavier composition.

### 3.6 $\delta^{13}C$ in the ocean

$\delta^{13}C$  is of interest to paleoclimatologists, but it is much more complex than  $\delta^{18}O$ , as C is a basic component of many geological and biological processes that constitute the biogeochemical carbon cycle.

The carbon cycle in the ocean is strictly related to the work of palaeoclimatology and paleoceanography; however, the  $\delta^{13}C$  commonly intermingles different sources (ocean itself and the outer part of the ocean, e.g., the atmosphere or mainland).

The ocean hosts many C compounds, both organic and inorganic. And the deep ocean is much more capable than the atmosphere and the shallow ocean, as it holds more than 95% of total fluid C that can be released into the atmosphere. Also, the atmosphere can provide and transfer carbon to the ocean; the continuous exchanges between the atmosphere and the ocean make the ocean often described as the atmosphere’s “slave”.

Therefore, what happens in the atmosphere is largely controlled by the dynamics of the ocean. As the ocean is a huge reservoir of carbon, this carbon can be subdistributed into smaller reservoirs that reside in the ocean:

#### 1. POC (Particulate Organic Carbon)

A small amount of carbon is resident in the ocean as individual living life, e.g., fishers. Having a quality of 20Gt and the fermentation will generate  $CO_2$ .

## 2. DOC (Dissolved Organic Carbon)

700Gt is represented by the DOC. The carbon is dispersed as tiny particles of organic matter in the ocean. They can refer to amino acids and proteins; some are molecular size but also have some small species of animals or vegetables. This large amount of carbon can be employed by many animals that filtrate the water to feed on themselves.

## 3. DIC (Dissolved Inorganic Carbon)

The largest amount of carbon (37,000Gt) is stored as inorganic compounds, like CO<sub>2</sub> or mineral compounds. Some small crystals disperse to the ocean, e.g., crystals of calcite or aragonite.

The average  $\delta^{13}\text{C}$  of DIC is around 0 (i.e., SMOW); however, it changes in space and time based on the following:

### 1. local biological productivity;

The higher the local biological productivity, the fractionation will be stronger, and the higher the seizing of light CO<sub>2</sub> from the water column.

### 2. photosynthesis/respiration balance;

The respiration process recycles the organic matter, and then algae employ again the light isotopes to form organic matter.

### 3. ocean circulation.

Transportation of carbon in the global or local sea.

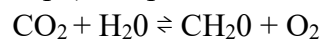
### 4. fluxes of carbon from the mainland.

In the ocean, there are a lot of photosynthetic creatures, e.g., algae. 90% of organic carbon from photosynthesis provided by the plants is recycled by aerobic bacteria virtually immediately into the photic zone; only part is digested by chemobacteria into the oxygen minimum zone at the bottom of the photic zone. Very little reaches the seafloor, which is void of organic matter and abnormal conditions only during the position of black shales or sapropel.

Phytoplankton (mostly C<sub>3</sub>) efficiently fractionate the DIC, simply taking from the water the preferential CO<sub>2</sub>, composed of light carbon and oxygen. These light components are transformed into organic matter; hence, the organic matter produced in the photic zone will be generally characterised by light isotopic signals. The surface water, accordingly, is enriched in heavy isotopes, especially carbon. And this carbon can be effectively employed in forming shells rich in heavy carbon with respect to ambient seawater, especially with respect to the biomass that is first generated. As these shells would subsequently sink and be deposited on the sea floor, there are huge amounts of sediments made of calcium carbonate and likely to be heavy isotopic.

Part of the ocean-atmosphere CO<sub>2</sub> exchange is driven by biotic activity. It is sustained by two biological pumps:

### 1. organic carbon pump (adsorption of CO<sub>2</sub> from the atmosphere to the ocean)

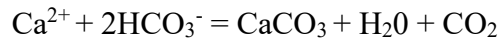


By photosynthesis, organic matter can be created by plants in the photic zone; most organic matter produced here is recycled and kept in the upper part of the water



column, with only very weak fluxes of organic matter down to the bottom of the sea.

2. calcium carbonate pump (release of CO<sub>2</sub> from the ocean to the atmosphere)



By secretion of shells, the flux of carbonate to the seafloor releases CO<sub>2</sub> to the atmosphere or can be employed by photosynthesis.

Both pumps provide the flux of carbon that is direct to the seafloor, the flux from the organic carbon pump is extremely weak, while the carbonate flux from the calcium carbonate pump is intense.

Clearly, δ<sup>13</sup>C is controlled by biological activity rather than temperature and sea level. A certain correlation may exist between δ<sup>13</sup>C and δ<sup>18</sup>O. This depends on the carbon cycle, which drives the concentration of atmospheric CO<sub>2</sub>.

Biota can provide a significant change in the global distribution of carbon and sedimentary conditions, e.g., under the anoxic condition that can provide persistence of carbon into sediments; otherwise, the organic matter may be destroyed by oxidation and then free into the water column. Also, inside the ocean, the distribution of carbon is very complex, vertically and horizontally according to the patterns that are related to the ocean circulation to redistribute original elements which are controlled by life.

For example, close to the coast, there may receive not only the flux of carbon from the upper part of the water column but also some vegetable debris (very light in its isotopic composition) that comes from the continent; these fluxes will mix with the composition flow which accumulates at seafloor under the form of inorganic sediment. Therefore, lots of factors collaborate in shaping the isotopic curve in a coastal region or others that are different from the open ocean setting.

In addition to having a complex δ<sup>13</sup>C distribution in different ocean areas, δ<sup>13</sup>C also shows a vertical gradient in the ocean (Fig. 3.6.1), mainly based on local biological productivity and photosynthesis/respiration balance. In the photic zone, many animals feed on the organic matter made of light carbon, then transfer and release into the seawater in the form of CO<sub>2</sub>, which contains light isotopes. The seizing and releasing of <sup>12</sup>C forms the oxygen minimum zone, which corresponds to the lightest value of δ<sup>13</sup>C, while the upper part of the photic zone has the “heavy” δ<sup>13</sup>C, up to 3‰, due to the isotopic fractionation produced by plant photosynthesis. Furthermore, the measurement of the composition of shells that live in this area also shows a high δ<sup>13</sup>C value. In the deep ocean, as many small animals, e.g., benthic foraminifera, live at the bottom of the sea and feed on very weak organic flows that escape from the oxygen minimum zone, by respiration, the light CO<sub>2</sub> is free into the bottom water. This allows us to measure a slight decrease in δ<sup>13</sup>C value (close to 0‰ at this point). And the shells form there would be made by the light CO<sub>2</sub>.

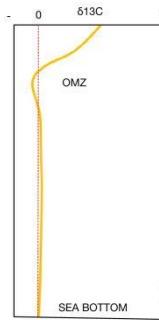
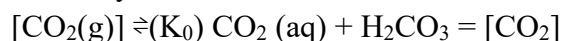


Figure 3.6.1: the vertical gradient of  $\delta^{13}\text{C}$  in the ocean.

$\delta^{13}\text{C}$  also links to the ocean circulation, deep ocean waters drain  $\text{CO}_2$  and enrich in  $^{12}\text{C}$ , and their  $\delta^{13}\text{C}_{\text{DIC}}$  decreases as time pass. The “young water” forms in the upper part of the ocean, which has heavy isotopic composition, will be rich in oxygen and relatively poor in  $\text{CO}_2$ . The flow then sinks to the bottom of the basin and creeps around the ocean before being raised to the surface. As the water moves through the bottom, its content changes dramatically: below the photic zone, the water loses oxygen by the respiration of animals living in the deep ocean, and this water will also become more affluent in  $\text{CO}_2$  in time. The isotopic composition of water becomes lighter consequently. For example,  $\delta^{13}\text{C}_{\text{DIC}}$  in the deep northern Pacific is approximately 1‰ “lighter” than the deep northern Atlantic. Atlantic is a new water mass forming and sinking both in the extreme south and north of the Atlantic area, representing “young” water; while in the Pacific, there is no sinking but only the strong upwelling, representing the resurfacing of “old” water.

The atmosphere and ocean exchanges mainly occur as in-out fluxes of  $\text{CO}_2$  as gas is volatile and can move fast from the absorbed efficiently by the ocean and release  $\text{CO}_2$  into the atmosphere as well, the solubility of which depends on temperature, local atmospheric pressure and salinity. The mechanism controlling the  $\text{CO}_2$  ocean-atmosphere exchange is known as the *solubility pump*, which provides the prevailing direction of the fluxes, which is toward the atmosphere or ocean. The *solubility pump* follows Henry’s Law:



where,  $K_0 = \text{CO}_2$  solubility (Weiss, 1974);

$[\text{CO}_2(\text{g})] =$  the concentration of gaseous  $\text{CO}_2$ ;

$[\text{CO}_2] =$  the concentration of  $\text{CO}_2$  in seawater

In modern oceans, the ratio between  $[\text{CO}_2(\text{g})]$  and  $[\text{CO}_2]$  is approximately 1:50. The law implies that the concentration of gaseous  $\text{CO}_2$  in the atmosphere is related to the concentration of  $\text{CO}_2$  stored in seawater, based on the solubility of  $\text{CO}_2$  in that specific condition. For example, the solubility of  $\text{CO}_2$  increases with decreasing temperature.  $\text{CO}_2$  gas can be absorbed into the ocean or other liquids as the aqueous form  $\text{CO}_2$  and carbonic acid ( $\text{H}_2\text{CO}_3$ ), which is unstable in natural conditions and destroyed in a few seconds, revert to  $\text{CO}_2$  and water.

This relationship regulates the dissolved inorganic carbon of the ocean (DIC). Dissolved  $\text{CO}_2$  occupies just 1% of the DIC in the ocean, but it is still 50 times greater than gaseous  $\text{CO}_2$ . Bicarbonate ion ( $\text{HCO}_3^-$ ) is the most abundant carbon

component in DIC, with 91%, and carbonate ion ( $\text{CO}_3^{2-}$ ) takes up roughly 8% of the DIC. The amount of carbonic acid ( $\text{H}_2\text{CO}_3$ ) is virtually negligible, less than 0.003% of DIC. The relative distribution of these components may change in time according to the changes in the chemistry of the global ocean and consequently provides many effects on the global climate system.

The atmosphere and ocean exchanges occur everywhere when wave breaks, forming a large number of foams which are small particles of water that reach the lower part of the atmosphere. This is a mechanical incorporation of the intake of  $\text{CO}_2$  and the other compound of the atmosphere. However, there are also presences of specific areas that have an effective massive intake or uptake of  $\text{CO}_2$ . The major part of the global intake of  $\text{CO}_2$  from the atmosphere to the ocean occurs at high latitudes, close to the polar areas. Cold surface waters here create the maximum  $\text{CO}_2$  solubility;  $\text{CO}_2$  is seized from the atmosphere, sinks and is transported to the bottom of the sea. Uptake and release of  $\text{CO}_2$  in correspondence to the area of upwelling, which usually takes place at the equator where the convergence between the trade winds.  $\text{CO}_2$ -rich waters are brought up to the top of the water column, and deep waters warm up and decrease the  $\text{CO}_2$  solubility to induce  $\text{CO}_2$  release.

The *Revelle factor* is an indicator of  $\text{CO}_2$  uptake or intake, defining how much atmospheric  $\text{CO}_2$  can move to solution into the mixed surface layer:

$$R = (\Delta[\text{CO}_2] / [\text{CO}_2])_{\text{atm}} / (\Delta\text{DIC} / \text{DIC})_{\text{sea}}$$

Where: R = Revelle factor (range between 8 and 15)

$\Delta[\text{CO}_2]$  = the change in the concentration of  $\text{CO}_2$

$(\Delta[\text{CO}_2] / [\text{CO}_2])_{\text{atm}}$ : a potential change in the concentration of  $\text{CO}_2$  with respect to the normal standard conditions in the atmosphere.

Since the ocean is resistant to the pressure of the atmosphere, DIC is always smaller than  $\Delta[\text{CO}_2]$ : if  $[\text{CO}_2]$  doubles, DIC increases by 10%. Revelle factor has higher values when located in higher latitudes, especially around Antarctica, with around 15; thus, there is almost no chance to release  $\text{CO}_2$  to the atmosphere, but only to receive  $\text{CO}_2$  from the atmosphere and transfer it into sinking water. The opposite is found in warmer regions, namely mid and low latitudes, the values there are lower. DIC composes of three components:  $\text{CO}_2$ ,  $\text{HCO}_3^-$ , and  $\text{CO}_3^{2-}$ . The system tends to work in equilibrium; if one component changes, it may experience a change in the concentration of other components, e.g., whenever the amount of  $\text{CO}_2$  dissolved in the ocean rises, we will observe a diminishing in the concentration of carbonate and a slight increase in  $\text{HCO}_3^-$ , the subsequent reduction happens in ocean pH. The relationship that links these three components shows that depending on the pH of the water, the composition of DIC varies. For example, once the amount of  $\text{CO}_2$  increases, saturated water with  $\text{CO}_2$ , is at the point the acidic conditions (which means the  $\text{CO}_3^{2-}$  ion would not be preserved in the ocean and there is no chance to precipitate or preserve carbonate) are created. Nowadays, scientists are particularly concerned about the possible future acidification of the oceans, especially for those animals that produce carbonate shells or aragonite shells because of the increase in  $\text{CO}_2$  emissions due to human activities. However, there is currently much debate on this discussion, based on the fact that the oceans tend to be in alkaline conditions

(pH at around 8) and that even an increase in CO<sub>2</sub> levels will not change their pH from always being greater than the threshold 7, so there is no possibility that carbonates in the oceans will dissolve.

Surface water around the world has a wide range of different pHs, higher latitudes are characterized by high values of pH, while equatorial regions observe a lower pH. In some regions, the surface pH of the ocean varies seasonally, and values can show a fluctuation of 1.6 from winter to summer, which means that there is a big change in the chemistry of water that is related to local temperature, river discharge (potentially variation, usually below 7), human case and soil.

The total alkalinity of a water mass depends on the difference between anions concentration and protons:

$$TA = [\text{HCO}_3^-] + 2[\text{CO}_3^{2-}] + [\text{B(OH)}_4^-] + [\text{OH}^-] - [\text{H}^+]$$

River runoff provides huge amounts of anions (in the order of 10<sup>12</sup> kg/year) which have a basic affinity, thus, the ocean remains basic nevertheless. Usually, tropical environments have thick shells made of calcite or aragonite as the water is basic with respect to the water at high latitudes, providing a favourable environment for carbonate deposition.

By comparing the addition of acid to pure water and marine water, it is clear that DIC buffers any change in water pH: in ultrapure water (DIC = 0), [HCl] → [H<sup>+</sup>] + [Cl<sup>-</sup>] in a 1:1 ratio, protons generated by dissociation of acid are not absorbed, which means nothing to buffer the concentration of protons; in marine water (DIC > 0), HCO<sub>3</sub><sup>-</sup> and CO<sub>3</sub><sup>2-</sup> adsorb protons (H<sup>+</sup>), the buffering effect of seawater is strong, as about 330 times more effective than common water.

## 4. Foraminifera

### 4.1 Biological characteristics

Foraminifera is an old group of protozoa that arose in the oceans at ca. 500 Ma. As fragile single-celled organisms, they evolved the ability to secrete calcium or silica to form a test with pores (one large or multiple fine pores) to protect themselves. Protoplasm can protrude from the pores, giving rise to amorphous protrusions outside, known as pseudopods. Foraminifera rely on these pseudopods for feeding and movement. The morphology of foraminifera is diverse and can be divided into three main groups according to the arrangement of their tests: unilocular, bilocular and multilocular test, each of which has different subgroups and arrangements, which results in a wide variety of test shapes. In terms of test composition, foraminifera have two types: those that form by secreting their calcium carbonate and those that form test by secreting an adhesive to bond to surrounding debris that can be taken away. Therefore, the tests of most foraminifera are mainly calcareous or colloidal in composition and are able to preserve for long periods in the stratigraphy.

To date, researchers have discovered and studied around 1,400 species of foraminifera. They are widely distributed and are found in waters around the world, and the stratigraphic distribution ranges from the Cambrian to the present. They are artificially subdivided in:

1. planktic foraminifera, is the most omogeneous group among foraminifera.
2. large benthic foraminifera, consists of benthic forms larger than 1mm. They usually show complex test structures (e.g., Nummulites) and preferentially thrive in tropical to subtropical environments. They can be lithogenic (Nummulites banks).
3. small benthic foraminifera, consists of benthic taxa usually smaller than 1 mm. They usually show simple test structures.

The vast majority of modern foraminifera are marine, with only a few living in semi-saline environments such as lagoons and estuaries, and a smaller number of broad-saline ones that can live in brackish water above normal salinity, while very few in freshwater, such as some individual species of the Lagynacea. They can be divided into planktonic and benthic species depending on their level of activity in the water column, with benthic species predominating in the early years; planktonic foraminifera did not appear until after the Mesozoic. The main factors affecting the growth, reproduction and distribution of foraminifera are water temperature, depth, salinity, the availability of suitable food and oxygen.

Foraminifera are an important link in the marine food chain. Their main food items are diatoms, bacteria, and crustacean larvae, with some particular species feeding on sand particles. As foraminifera are an essential component of plankton, they are also an important food source for most marine organisms.

#### 4.2 Applications in Paleoceanography

Foraminifera have important applications in many areas of scientific research, such as biostratigraphy (due to the characteristic high evolutionary rate of foraminifera, it mainly focuses on planktic and large foraminifera), lithogenic study (large foraminifera on shelves; planktic foraminifera in the pelagic domain) and paleoenvironmental reconstruction (paleobathimetry, paleotemperature and ocean chemistry). Here we focus on its application to paleoceanographic research.

Foraminifers fractionate  $\delta^{18}\text{O}$  in equilibrium with the ocean: the  $\delta^{18}\text{O}$  of their tests reflects the temperature and  $\delta^{18}\text{O}$  of seawater (i.e.,  $\delta_{\text{sw}}$ ). And  $\delta_{\text{sw}}$  varies in the geologic time based on the extent of continental ice caps, which is a global signal and the environment (e.g., temperature, salinity and runoff). Suppose scientists move to other animals as a proxy to make the calculation. In that case, they have to deal with many fossils that do not precipitate their calcite in equilibrium with seawater, that is difficult to correct.

As we mentioned above, at the beginning of the paleoceanographic study, the first one to link isotopes in the shells of marine organisms to changes in temperature was Urey; the species he chose were bivalves. However, the research has many problems with the bivalve as an archive. The use of palaeontological fossils to determine the relative geological age of strata is a standard tool used by scientists, while bivalves are attributed to very poor biostratigraphic significance since they have a slow evolutionary rate and the amount of them cannot help scientists discriminate the age of sediments. Also, bivalves are uncommon and discontinuous in terms of abundance in the stratigraphic records, their distribution is commonly controlled by sedimentary facies, thus researchers who want to use them as a proxy

to reconstruct the past climate or environmental conditions have to find the right interval time with suitable facies so that may collect a proper number of proxies. The biggest problem is that bivalves are not in equilibrium in isotopic fractionation when they secrete their shells for many instances, there are no direct responses between the composition of their shells and ambient seawater.

In 1968, the DSDP project began, and large numbers of foraminiferal samples from deep-sea sediment cores gave a more favourable tool for reconstructing paleotemperatures. The first one to be used as a proxy was planktic foraminifera which live in the photic zone and represent 99% of the total amount of microfossils that can be found in the sediments at the seafloor. Compared to bivalves, planktic foraminifera have been abundant in the stratigraphic records since the end of the Jurassic and is lithogenic (for many instances, planktic foraminifers are the rock itself). Moreover, planktic foraminifers are independent of the sediments composition since they live in the water column and are easily transported to the open ocean or coast. The excellent preservation and diversity of foraminifera from ancient times to the present provide a natural advantage in biostratigraphic studies. Because the time from origin to the extinction of a species of foraminifera is instantaneous in relative terms of geological time, the generic classification of foraminifera can be used as a precise guide to chronostratigraphy, and foraminifera can become good biostratigraphic indicators. Moreover, foraminifera are indicators of the marine environment, widely used in studies of global change on long-time scales in the oceans. As previously described, foraminifera secrete calcite or aragonite to form protective tests. When they grow, their tests also grow in size with the secretion of calcium carbonate and contain a ratio of stable isotopes which is most of the time in equilibrium with ambient seawater (for both planktonic and benthic species). Foraminifera have a very short life span, mostly of a few days to a few weeks. After the foraminifera die, the tests sink to the sea floor and are gradually buried within strata, recording the isotope ratios of the seawater at that time. Therefore, researchers just need to calculate the offset (the difference between the composition of the seawater and the measured composition of calcite or aragonite which is commonly heavier than the water) that is constant independently of the temperature. Thus, compared to bivalves, planktonic foraminifers are reliable and open a window for the scientific community in reconstructing past climates. Later, Urey discovered the shortcomings of using planktonic foraminifera in calculating temperatures, as we said before. Instead of using planktonic foraminifera, benthic foraminifera which live in almost constant temperatures in time, are more suitable for reconstructing past temperatures and can also be used to evaluate the glacioeustatic effect. Theories were developed and experiments were carried out by Shackleton.

#### 4.3 Benthic foraminifera

The benthic foraminifera are usually slow-moving on the sea floor, with only a few growing in place. They can be subdivided into suspensivorous and detritivorous according to their feeding modes or their living position in relation to the seabed.

In the latter case, a distinction can be made between epifaunal and infaunal benthic foraminifera: the former live on the seabed, while the latter live sunken in the substratum. The vertical distribution of infaunal foraminifera is influenced by two limiting factors: the amount of organic matter contained in the sediment and the presence of oxygen (as shown in Figure 4.3.1). And the availability of organic matter is regulated by the flow of nutrients and the rate of decomposition.

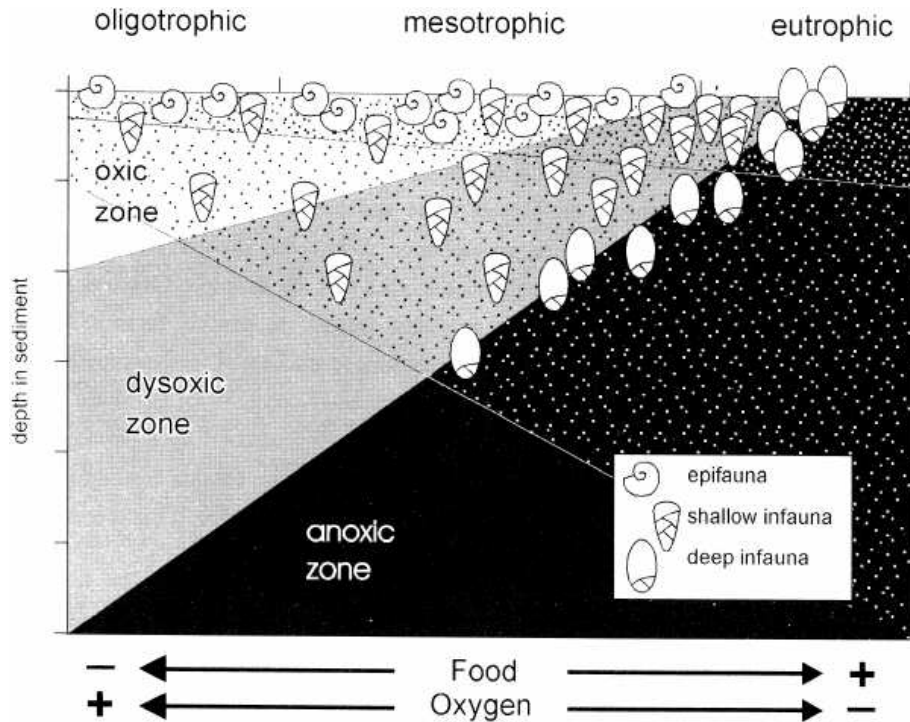


Figure 4.3.1: Distribution of different species of benthic foraminifera in sediments and association with oxygen.

The sensitivity of deep-sea benthic foraminifera to environmental change and the close correlation of their test stable isotopes and trace elements with seawater properties make them a powerful tool for the study of paleoceanography. Through a series of studies over the years by the scientific community to reconstruct the paleoclimate (also described in Chapter 3), among the different proxies to work on, most of the benthic foraminifers (depending on the species) are the most reliable paleoclimatic record available to date, providing relatively precise and credible information.

#### 4.4 *Uvigerina peregrina*

In our case study, the *Uvigerina peregrina* (Cushman, 1923) benthic foraminifera from PCS core, which was also one of the foraminifera used in the study of Reghellin as a comparison, was used to obtain  $\delta^{18}\text{O}$  and  $\delta^{13}\text{C}$  data for analysis and comparing.

*Uvigerina peregrina* is a species that is characterized by a high spatial distribution and can be found from shallow waters (-100m) to abyssal plains at carbonate compensation depths (ca. -4,500m). Also, the species is easily identifiable due to their hyaline calcite tests with elongated shape (about 2.5 times long as broad),

widest in the middle, and rounded ends. Thus, they are one of the most commonly studied benthic foraminifera used by scientists and possibly offer the most reliable biotic archive of the paleoclimatic and paleoenvironmental conditions at the seafloor. The ideal microhabitat for *Uvigerina peregrina* consists of abundant fluxes of organic matter and low oxygen concentration (these conditions vary from the most marginal to abyssal depths); therefore, these organisms are often related to upwelling areas (Altenbach and Sarnthein, 1989).



Figure 4.4.1: *Uvigerina peregrina* (from Cushman, 1923).

## 5. Materials and methods

### 5.1 Brief introduction

In order to minimize the other factors that may have affected the acquisition of isotopic data and to highlight only the differences in the results obtained by the different mass spectrometers, we have followed the entire process of Reghellin's experiment in 2010, including sample pre-processing, picking, mass spectrometer analysis, as closely as possible. All experimental procedures were carried out at the Geosciences Department of the University of Padova. Isotopic analysis was carried out on specimens of the benthic foraminifera infaunal *Uvigerina peregrina* recovered from 265 samples by four different students (CCR 700 - CCR 770 by Morelli; CCR 771 - CCR 830 by Lin, i.e., the author; CCR 831 - CCR 890 by Shi; CCR 891 - CCR 964 by Wang). Because the four experimental data acquisition processes were conducted simultaneously and identically, only the author's process is described here, and many thanks to the other three students who provided their data, making our comparison data richer and obtaining relatively credible comparison conclusions.

### 5.2 Pre-pick preparation

In order to pick the foraminifera that were needed for the study from the samples, a four-step pre-treatment process was carried out in the Micropaleontology laboratory, including initial weighing, washing and filtering through sieves, drying, removing in plastic bags and a second weighing (i.e., the "dry weight" as marked thereafter).

Sixty samples were taken from the PCS core samples stored at the Department of Geosciences and previously preserved in individual plastic bags labelled with the CCR ("Carota Crosia") number. Sixty samples were numbered CCR 771 to CCR 830, corresponding to the order of samples from shallowest to deepest.

Preliminarily, samples were initially weighed with a standard weight of approximately 50.0 grams and packaged. This step was carried out on a balance to



one decimal place. At the same time, the remaining portion of each sample was collected in a separate plastic bag after the initial weighing, also marked with the corresponding CCR number, as a “backup” in case of any errors during the experiment and also for future analyses. It should be noted here that due to the need to retain a certain mass of “backup” samples (probably at least 20 grams), the initial weighing did not reach the standard weight of around 50.0 grams for some samples that originally had a low total mass. The CCR 777, for example, has an initial weight of only 28.3g because it has a very low total weight: 46.4g.

After the initial weighting and packaging step, the individual samples with about 50.0g initial weight were placed inside beakers, and enough water was added to submerge the samples, which were left to soak for approximately 16 hours in order to promote complete disintegration. Subsequently, each sample was poured into sieves carefully for washing and sieving. Two stacked sieves were used: the upper with a mesh size of 2mm (to facilitate the cleaning of the sample, especially for larger particles such as twigs and small stones, and to prevent spillage due to the smaller bore size of the sieve below), while the sieve below with a denser mesh of  $63\mu\text{m}$  in order to eliminate the clay fraction of the various samples. The washing and sieving process by means of using a water jet gently and repeatedly flushing the sediment poured into the sieves until the clay fraction is completely removed, i.e., until the wash water flowing out of the sieves is free of suspended material, can be looked entirely transparent to the naked eye. At the end of the washing and filtering step, the residual fraction in the  $63\mu\text{m}$  sieve was rinsed with deionised water to remove possible lime residues; next, these remaining sediments were transferred to a drying bowl labelled with the corresponding CCR number.

The drying step was carried out in an oven in the lab, where drying bowls with the remaining fraction were placed and then dried at  $50^{\circ}\text{C}$  for about 12 hours until they completely dry. Then, the particles in the bowl were gently swept with a brush onto a clean sheet of paper to facilitate their later transfer to an antistatic plastic bag for the second weighing. There were occurrences where the fine powder particles attached to the wall of the bowl were too strong to be removed by the brush, but as the final study was on foraminifera, the larger particles were better transferred by the brush; therefore, the powder particles missed on the bowl would not have affected the final results.

The second weighing was done using an analytical balance, which is accurate to four decimal places. Before each weighing, the empty antistatic plastic bag was first placed on the balance for zeroing, in order that the mass subsequently weighed was exactly the mass of the dry sample obtained. After reading the dry weight of each sample, the plastic bag containing the sample was tightly sealed with tape and marked with the sample CCR number, the respective values of the initial weight and dry weight of the sample, and the smallest pore size of the sieve used in the filtering, i.e.,  $63\mu\text{m}$ . This weight information can be found in the table at the end of the article.

In addition, the cleaning process after each use of the sieves and drying bowls is critical, as the equipment is reused. If any sample debris remains from the last

experiment, it will be confused with the product of subsequent experiments and may have a misleading effect on the final isotope results. Therefore, two main methods were used throughout the pretreatment process to prevent this problem:

1. soaking the denser sieve (i.e., the  $63\mu\text{m}$  sieves) in a methylene blue solution for one minute before washing it, so that any residual foraminiferal staining from the last experiment could be marked in blue and easily avoided in the subsequent microscopic picking.
2. brush the sieve carefully with a cleaning solution and rinse it repeatedly with a stream of water after each use; also, wash the drying bowl with a stream of water after each use until any particles that may have adhered to the walls of the bowl have disappeared.

### 5.3 Picking

The picking process means picking out the foraminifera *Uvigerina peregrina* from the sieved and dried fraction previously collected in the plastic bags. The processes were done in the Microscopy teaching laboratory of the Department of Geosciences. These fractions were first sieved through a  $128\mu\text{m}$  aperture sieve (Fig. 5.3.1), poured into the sieve, covered and gently shaken. The lid was then opened and the samples in the sieve were slowly poured into a plate with reference grids to identify the position of the particles (Fig. 5.3.2). A coarse brush (Fig. 5.3.1) was used at this point to remove some particles that had not been poured out.



Figure 5.3.1: the  $128\mu\text{m}$  aperture sieve (left) and the coarse brush (right) used.

The plate was placed under an optical microscope; the *U. peregrina* among the samples could be observed by moving the plate and collected using a fine brush lightly moistened with deionized water (to increase the adhesion to the fibres). Subsequently, the collected organism was collected in a sealed sample holder and labelled with the CCR number and specimen's name. (Fig. 5.3.2)

During the picking process, we also recorded the observation of each sample under the microscope, including the quality of the desired foraminifera (i.e., *U. peregrina*), their quantitative abundance and the overall characteristics of the samples observed (this information is also presented in the table at the end of the article), to facilitate subsequent research and analysis. When describing relative quantitative abundance, we use “abundant” to refer to *U. peregrina* occupying 70% or more of all particles in the sample; “present” to refer to occupying between 50% and 70%; “poor” to represent less than 50% but still present; “absent” means that no tests of this type of foraminifera could be found in the sample at all. Of the 60 samples observed, all

of the analysed samples are defined as less than 50% (poor) except CCR 807 and CCR 817 which are more than 50% and described as “present”, also, CCR 827 - CCR 830 which is “absent” as here enters the sapropel layer. For the description of the test quality of foraminifera, we use “good” for complete and clean tests; “clean”, for clean but broken tests; “bad” for badly broken tests; “dirty” for unclean tests. During the observation and picking process, the tests in all samples (except CCR 827 - CCR 830) were in good condition, so we marked them all as “good”.

It should be noted here that in Reghellin’s study, a comparison of isotopic results obtained for the two main test sizes (i.e., 150 - 250 $\mu\text{m}$  and 250 - 355 $\mu\text{m}$ ) of *U. peregrina* was carried out and showed an offset between the two sets of results (Fig. 5.3.3), particularly for the carbon stable isotopes, where there was a clear correlation with the test size of the foraminifera used (larger foraminiferal tests correspond to heavier values), while this was not a significant difference for the oxygen stable isotopes and could be neglected. The selection of tests of foraminifera with relatively similar dimensions was therefore important for subsequent data acquisition. Reghellin chose mostly 250 - 355 $\mu\text{m}$  sized foraminifera (some smaller-sized fractions, i.e., 150 - 250 $\mu\text{m}$  range, were used in subsequent mass spectrometer analyses to make up the mass) in order to avoid the effects of isotopic fractionation changes during foraminiferal growth on the results. Therefore, in our experiments, we have also imposed requirements on the size of the foraminiferal tests selected, and we excluded smaller-sized foraminifera because they might lead to insufficient material quality for subsequent isotopic analysis, and also reduction of size-related fractionation effects (this is more prominent in juvenile forms of foraminifera). At the same time, as our sample suffered from insufficient numbers (as recorded in the table at the end of this article, the majority of the samples have a “poor” quantitative abundance), a proportion of smaller sizes were also mixed in with the foraminifera picked, and the addition of small-sized tests samples is not entirely consistent with that in Reghellin’s experiment; thus, we consider that our sampling did not achieve strict control of the 250 - 355 $\mu\text{m}$  range, a problem of bias present that needs to be taken into account at a later stage of comparison.



Figure 5.3.2: the optical microscope (middle), the plate with reference grids (under the microscope), the fine brush used (right side of the microscope), the bottle of deionized water (left side of the microscope) and the sealed sample holders (top left).

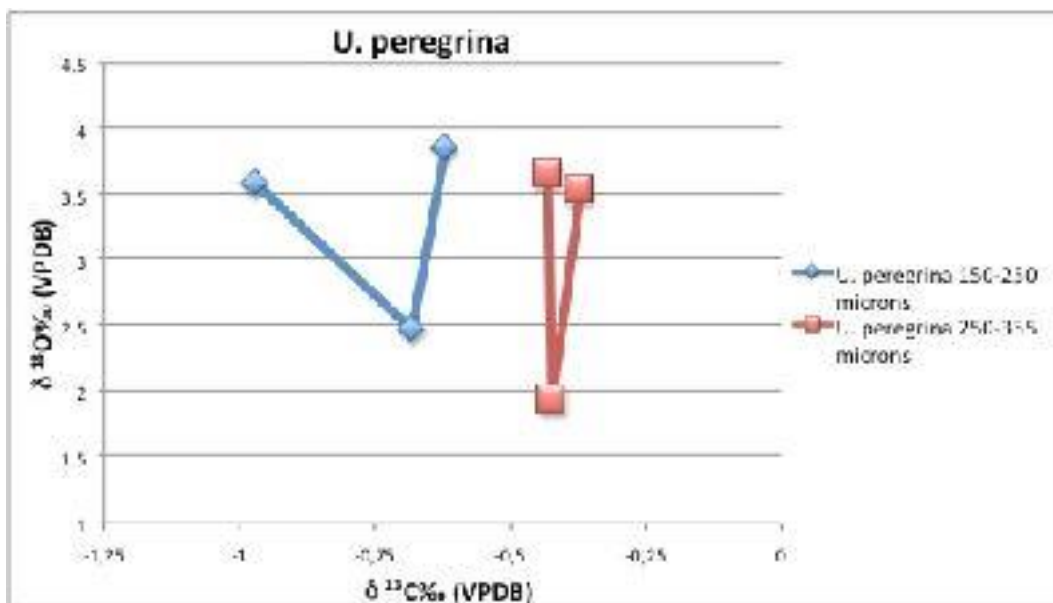


Figure 5.3.3: a comparison of isotopic results obtained for the two main test sizes (i.e., 150 - 250 $\mu\text{m}$  and 250-355 $\mu\text{m}$ ) of *U. peregrina*. The blue line in the graph represents data obtained from tests of foraminifera with sizes 150 - 250 $\mu\text{m}$ , and the red line represents sizes 250 - 355 $\mu\text{m}$  ones, we can observe a clear deviation between the two sets of data. (from Reghelin, 2010)

## 6. Mass spectrometer

### 6.1 Brief introduction

The mass spectrometer is able to measure the relative abundance of the various isotopes of a given sample. It, therefore, allows the separation of mixtures of ions obtained by ionizing the sample molecules through a beam of electrons by virtue of their mass-to-charge ratio using magnetic fields.

Isotope Ratio Mass Spectrometer (IRMS), the most widely used spectrometer, allows for determining the intensity of ion beams generated by low amounts of CO<sub>2</sub> and measuring the abundances of stable carbon and oxygen isotopes. The main components of this instrument are an ion source, which can ionize the sample molecules and accelerate and focus the ions later; a mass analyzer, in which the ions previously separated as a function of their mass/charge ratio is conveyed by means of an electromagnetic field; a detector that identifies the ions and transforms this input into an electrical signal, subsequently amplified, which will then be interpreted by a computer.

## 6.2 Mass spectrometer experiments by the University of Padova (using the Delta V Advantage)

The instrument we used to analyse the stable isotopes of oxygen and carbon is an IRMS (Isotope Ratio Mass Spectrometer) Thermo Scientific Delta V Advantage (Fig. 6.2.1), operating in continuous flow connected to GasBench II and is located in the Department of Geosciences of the University of Padova.



Figure 6.2.1: Thermo Scientific Delta V Advantage IRMS in the Department of Geosciences of the University of Padova.

Ten previously prepared foraminiferal tests for each sample were taken and manually loaded into 10ml round-bottomed borosilicate exetainers and tightly sealed by butyl rubber septa (Fig. 6.2.2).



Figure 6.2.2: 10-ml round-bottomed borosilicate exetainers (right) and the butyl rubber septa (top left).

The loaded samples were placed in a certain order in the sample rack (Fig. 6.2.3), where 72 exetainers were put in, including 56 exetainers with samples (i.e., CCR 771- CCR 827), 2 void exetainers (first and last position), 12 aliquots of an in-house standard for the analysis control (i.e., MAQ 1, normalized standard) and 2 quality assurance standards for the calibration (i.e., GR 1; they always placed in the same position in the sample rack, i.e., positions 28 and 61). (Figure 6.2.4)

Specifically: MAQ 1 (Marble Altissimo Quarry, “1” means among the different available samples, the very first one provided the best chemical analyses (the cleanest)) is a Carrara marble derived from the so called “cava di Altissimo”, a quarry that was owned by Michelangelo in person. GR1 derived from a metamorphosed sample of the Contrin formation (also is marble), recovered by a group of students during a Field camp (GR stands for group; GR1 because that group was the group number 1 among the others groups during the excursion). This marble had perfect isotopic values and so could be employed for the calibration of the mass spectrometer measurements. For subsequent linearity corrections, we weighted the standard to ensure that it is in the proper mass range: 200 - 250 $\mu\text{g}$  (most desirable range); 250 - 350 $\mu\text{g}$  (proper range); 180 - 200 $\mu\text{g}$  and 350 - 450 $\mu\text{g}$  (general range).



Figure 6.2.3: order of placement of samples and standards on the sample rack.

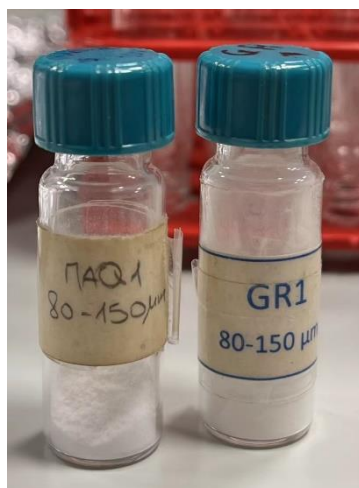


Figure 6.2.4: MAQ1 (left, for the analysis control; normalized standard) and GR1 (right, for the calibration). They both are Calcium carbonate.

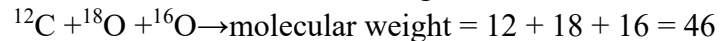
Initially, helium is injected into the exetainer at a flow rate of 120 ml/min by a double-hole needle that perforates the butyl rubber septa on the tube cap. This gas can replace the air present, which could distort the data obtained from the isotopic analysis; the duration of this first phase is approximately 4 to 5 minutes per sample. Then, the second stage is to react the samples with concentrated phosphoric acid ( $H_3PO_4 > 99\%$ ), which is automatically deposited in each exetainer using the autosampler and a stainless-steel capillary needle attached to an acid pump. The reaction takes approximately three hours; this is done in order to transform the calcite of the foraminifera tests into carbon dioxide and water:



At the same time, there has a second needle transfers the evolved gas into the GasBenchII driven by a small stream of He (0.5 -1ml/min).

After the water removal by Nafion traps, the produced  $CO_2$  from the last step is separated from other components using a gas chromatographic column which is heated to  $70.0^\circ C$ , and the peak corresponding to this  $CO_2$  is then passed through an open split into the mass spectrometer.

The CO<sub>2</sub> molecules obtained will be characterized by different molecular weights, depending on the different oxygen and carbon isotopes that compose them. The most commonly obtained combinations are:



On this basis, mass spectrometers are able to measure the masses of different molecules, and the most common configuration (i.e., those actually detected by the instrument) are <sup>12</sup>C<sup>16</sup>O<sup>16</sup>O (44), <sup>13</sup>C<sup>16</sup>O<sup>16</sup>O (45), and <sup>12</sup>C<sup>18</sup>O<sup>16</sup>O (46). “Heavier” configurations (e.g., <sup>13</sup>C<sup>18</sup>O<sup>16</sup>O) are very rare. Therefore, the measurements of the abundances of the stable isotopes is relating to the isotopic composition measured on the the standard reference sample (i.e., δ, which is described in Chapter 5.2). And all of our results are given as per mil (‰) deviation versus the international VPDB (Vienna Bee Dee Belemnite).

Meanwhile, according to previous research by scientists, the laboratory equipment we used provides us with many facilities:

1. the continuous-flow technology (i.e., the GasBenchII device we used here) can offers good internal and external precision for online isotopic measurements of calcite samples;
2. the autosampler equipped used with two needles allows the reaction time and the amount of acid used per sample are kept constant;
3. samples can be reacted at temperatures significantly higher than room temperature, which in conjunction with a heated GC column allows fast chromatographic separation of gas phases and hence high sample throughput.

### 6.3 Mass spectrometer experiments by Reghellin in 2010 (using MAT 252)

As we said in Chapter 1.1, some of the samples from PCS core were previously sent to the Department of Geology of the University of Stockholm (Sweden) after a series of pre-processing at the University of Padova, and they were isotopically analysed by a Finnigan MAT 252 isotope ratio mass spectrometer coupled also with a Finnigan Gasbench II device there.

There was two international standards and two in-house laboratory carbonate standards were used in this isotopic analysis, which namely are: NBS 19, IAEA-CO-1, Carm-1 and CaCO<sub>3</sub>\_Merck (Révész and Landwehr, 2002). Twelve standards (three for each type) were measured every time 48 analysis were performed on the study material.

A similar situation to ours occurred in this experiment, i.e., some of the samples were of insufficient quality when pick foraminifera in the 250 - 355μm size range only, so a proportion of the 150 - 250μm size foraminifera were added to these samples to ensure that the experimental samples were of sufficient quality, as we have previously mentioned.

## 7. Result and Discussion

We obtained the δ<sup>13</sup>C and δ<sup>18</sup>O data from -50.0m to -76.2m of PCS core, and



overlapped the data acquired by Reghellin at the same depth for easy comparison.

## 7.1 $\delta^{13}\text{C}$ curve and comparison

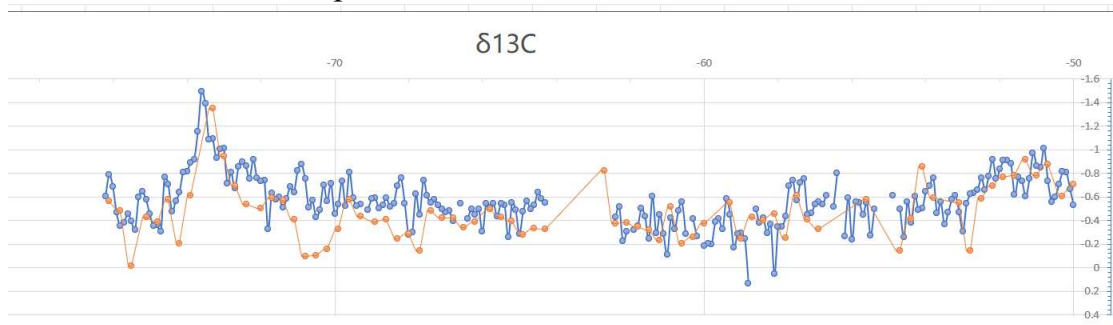


Figure 7.1.1: the  $\delta^{13}\text{C}$  curve obtained by Delta V Advantage IRMS in the Department of Geosciences of the University of Padova (blue); the  $\delta^{13}\text{C}$  curve obtained by MAT 252 IRMS in 2010 (orange).

It is straightforward to observe that the  $\delta^{13}\text{C}$  data records we obtained by Delta V Advantage IRMS largely match the data obtained from MAT 252 in 2010 (Fig. 7.1.1). The data we obtained for  $\delta^{13}\text{C}$  has a maximum value of 0.135304229‰ (corresponding to CCR 791), a minimum value of -1.493112526‰ (corresponding to CCR 938) and fluctuates mainly in the ca. -0.2‰ to ca. -1‰ range. Comparison with data obtained by Reghellin: the  $\delta^{13}\text{C}$  values of *U. peregrina* vary from -0.02‰ (PCS 96) to -1.35‰ (PCS 89), and oscillations are mainly between ca. -0.25‰ and ca. -0.75‰ (Reghellin, 2010).

As we said before, there are numerous factors affecting  $\delta^{13}\text{C}$  records and their interpretation is much more complex than that for  $\delta^{18}\text{O}$ ; therefore, with the limited data available, only some simple basic speculations can be made. Reghellin interpreted the large fluctuations (ca. -0.25‰ and ca. -0.75‰) of his  $\delta^{13}\text{C}$  curves as a result of variability patterns in primary productivity within the photic zone, corresponding to the data we obtained, the large swings (the ca. -0.2‰ to ca. -1‰ range) within the interval are equally prominent, as they could also be consistent with that speculation.

## 7.2 $\delta^{18}\text{O}$ curve and comparison

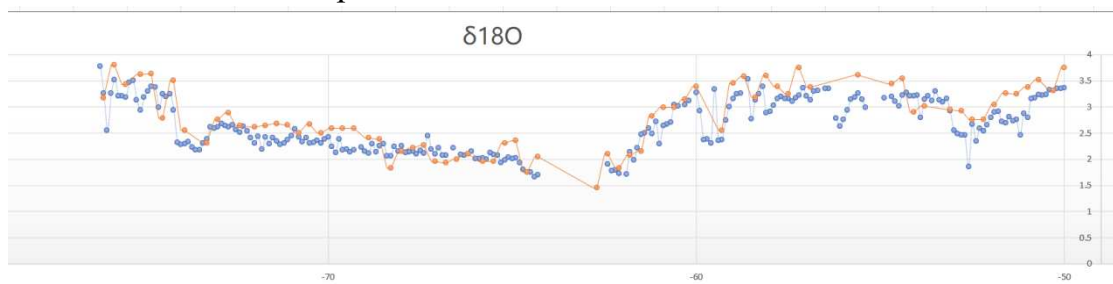


Figure 7.2.1: the  $\delta^{18}\text{O}$  curve obtained by Delta V Advantage IRMS in the Department of Geosciences of the University of Padova (blue); the  $\delta^{18}\text{O}$  curve obtained by MAT 252 IRMS in 2010 (orange).

It can be easily observed that the  $\delta^{18}\text{O}$  data records we obtained by Delta V Advantage IRMS also largely match the data obtained from MAT 252 in 2010. The two curves even match more effectively than the  $\delta^{13}\text{C}$  record curves above. The data we obtained for  $\delta^{18}\text{O}$  has a maximum value of 3.780989829‰ (corresponding

to CCR 964), a minimum value of 1.666108247‰ (corresponding to CCR 846), a maximum amplitude of 2.114881582‰ and a mean value of 2.645998709‰. Comparison with data obtained by Reghellin: the  $\delta^{18}\text{O}$  values of *U. peregrina* range from 3.81‰ (PCS 97) to 1.45‰ (PCS 55), with an average of 2.79‰ (when only the depth ranges from -50m to -76.2m are considered, i.e., PCS 1 - PCS 98) and a maximum amplitude of 2.36‰. (Fig. 7.2.1)

When considering a full comparison of our  $\delta^{18}\text{O}$  data with the isotopic composition of modern *Uvigerina* spp. in the eastern Mediterranean (Vergnaud Grazzini *et al.*, 1986), we can similarly interpret close to or less than 2‰ as indicative of an interglacial condition as Reghellin; and the same situation arises for the case where the maximum value of the interval data found in the Reghellin study is less than the average value (4.5‰) in last glacial maximum (LGM) suggested by Grazzini *et al.* Even, because the depth interval we were studying is somewhat shorter, our maximum value is less than 4‰ that of Reghellin, and therefore will be smaller compared to the value of 4.5‰. As for the maximum spread of ca. 2.115‰, it also exhibits the same situation as that obtained by Reghellin, which is much larger than that exhibited by *Uvigerina* obtained in the deep sea, i.e., about 1.5‰ (Shackleton and Opdyke, 1973).

As the PCS core represents upper slope or outer shelf conditions rather than a deep-sea environment, the indicator values for glacial and interglacial conditions should also be different from deep-sea conditions for ice ages and interglacial. Reghellin had identified values of 4‰ and heavier as indicators for full ice age conditions and values of 2‰ and lighter pointing to full interglacial conditions for this situation. With reference to these two indicators, Reghellin considered the  $\delta^{18}\text{O}$  values obtained by *Uvigerina peregrina* therefore records two main ice ages events (i.e., GP1-GP2 complex and GP3 interval), separated by a main interglacial phase (i.e. IP2). Of these, GP1 and GP2 are considered as one articulated and prolonged glacial stage, as there are no values among them that are able to reflect the full interglacial conditions, only a relatively small drop in data, labelled as a relatively warm minor event of *iPa*. Also, Reghellin marked the *iPb* event after the GP3 phase. (Fig. 7.2.2)

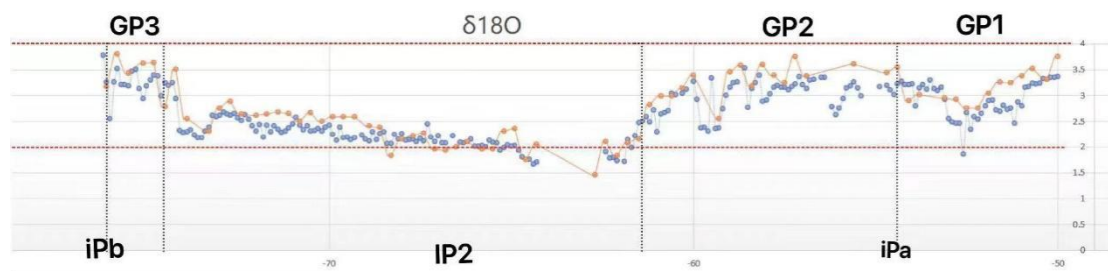


Figure 7.2.2: the two  $\delta^{18}\text{O}$  curves correspond to the events labelled by Reghellin.

We also overlap our curves according to the event phases labelled by Reghellin. (Fig. 7.2.2) Here it is very intuitive to see that the data we have obtained match very closely all the ice ages and interglacial events labelled by Reghellin before. In addition, the minor event “*iPa*” that Reghellin has identified according to their data, can be better observed in the data we obtained because of our higher resolution, in fact, the values we obtained in this interval are lower than those obtained by

Reghellin, that is further evidence of the presence of a “warm” small event here. Thus, the  $\delta^{18}\text{O}$  data we obtained strengthens the validation of the climate cycle and major events recorded in the PCS core as inferred by Reghellin, and improves Reghellin’s inference of the small warm events during the major glacial event GP1-GP2, supporting the idea that global ice volume changes can be reflected by benthic foraminifera *Uvigerina peregrina* (Shackleton and Opdyke, 1973).

### 7.3 Further discussion

We can clearly observe that there is a relatively large difference in the  $\delta^{13}\text{C}$  curve compared to the  $\delta^{18}\text{O}$  curve between the two different IRMS-generated data (this can also be seen in the comparison of the detailed analysis above), and we considered this should be due to the fact that in the picking step of the experiment, we did not follow exactly the range of foraminiferal test sizes chosen by Reghellin (i.e., 250 - 355 $\mu\text{m}$ ) as the insufficient sample available for selection. As we mentioned before, based on a small test done by Reghellin (Reghellin, 2010) on his test sample, carbon isotope ratios are strictly dependent on the size of the specimen tested, with larger specimens showing “heavier” values and vice versa. Conversely, offset in oxygen isotope data can be considered negligible. This result explains the discrepancy in our data very well. It also echoes Norris’ theory (Norris, 1996) that in order to minimise the variation in isotopic signal due to fractionation changes in foraminiferal growth and to establish consistent and reliable stable isotopic profiles, mass spectrometry experiments should be conducted in such a way as to ensure that the foraminiferal test samples used are of the same size range.

At the same time, a number of blank cases appear in our data sequence, resulting from two main causes: episodic influxes of coarse sands and silts (especially in full GP2 glacial event) or laminitic intervals which are no benthic foraminifera were found (i.e., CCR 827 - CCR 844, in other studies there has been determined as the sapropel-like layer). Comparing the gaps in Reghellin’s data, the locations where they occur are almost identical to those in the data we obtained. The laminitic intervals are considered to be formed during a period of extreme stratification of the water column and oxygen depletion at the seafloor. (Wang, 2023)

## 8. Conclusion

In order to compare the differences in the acquisition of isotope data of two isotope ratio mass spectrometers, MAT 252 and Delta V Advantage, which are very different in price but both commonly used in the field of geological research for isotope analysis, we propose as case study a stable isotope analysis on benthic foraminiferal *Uvigerina peregrina* tests from the lower part (i.e., from -50.0m to -76.2m) of the PCS sedimentary core (Lower Pleistocene, Calabria, Italy) which has been reconstructed also the stable isotopic data in 2010 by Reghellin for the very same stratigraphic interval using the MAT 252 mass spectrometer of the Department of Geology of the University of Stockholm (Sweden).

60 samples were washed, sieved, and cleaned following identical procedures, which ensured consistency with the procedures carried out in 2010. A continuous record

for  $\delta^{18}\text{O}$  and  $\delta^{13}\text{C}$  was reconstructed using the Delta V Advantage mass spectrometer at the Department of Geosciences of the University of Padova. After overlapping and comparing the data we obtained from the Delta V Advantage with the same depth data from Reghellin using the MAT 252, the following are our results:

1. In our comparative case study, the data curves obtained by the two different mass spectrometers were highly matched, with both oxygen stable isotope curves and carbon stable isotope curves. Thus, in the curves we obtain, we can likewise find the series of events and phenomenon inferred from the analysis of Reghellin, including:

1) The variability patterns in primary productivity within the photic zone which corresponds to the large oscillations of  $\delta^{13}\text{C}$ .

2) The maximum spread of  $\delta^{18}\text{O}$  curve (ca. 2.115‰) is much larger than that exhibited by *Uvigerina* obtained in the deep sea, i.e., about 1.5‰, corresponding to PCS core representing upper slope or outer shelf conditions.

3) The GP1-GP2 complex and GP3 interval, which indicate to ice age, and the interglacial events *iPa*, IP2 and *iPb*, with the indicator values for glacial (4‰) and interglacial (2‰) conditions defined by Reghellin considering about the PCS core representing upper slope or outer shelf conditions.

4) The blank cases appear in our data sequence, resulting from two main causes: episodic influxes of coarse sands and silts (especially in full GP2 glacial event) or laminitic intervals which defined as a sapropel-like layer.

2. As our experiments at the University of Padova have higher resolution data than the previous Reghellin experiments, with  $\delta^{18}\text{O}$  and  $\delta^{13}\text{C}$  values reaching nine decimal places and sampling every 0.1 m. Our data results can also be supplemented to improve the inferred event indicated by Reghellin: the minor event “*iPa*” that Reghellin has identified according to their data can be better observed in the data we obtained because of our higher resolution, in fact, the values we obtained in this interval are lower than those obtained by Reghellin, that is further evidence of the presence of a “warm” small event here.

3. There is a relatively large difference in the  $\delta^{13}\text{C}$  curve compared to the  $\delta^{18}\text{O}$  curve between the two different IRMS-generated data. Based on a small test done by Reghellin (Reghellin, 2010) on his test sample, carbon isotope ratios are strictly dependent on the size of the specimen tested, with larger specimens showing “heavier” values and vice versa. Conversely, offset in oxygen isotope data can be considered negligible. This result explains the discrepancy in our data very well. Thus, we considered this appearance of difference should be due to the fact that in the picking step of the experiment, we did not follow exactly the range of foraminiferal test sizes chosen by Reghellin (i.e., 250 - 355  $\mu\text{m}$ ) as the unavoidable problem which is insufficient sample available for selection. It also can echo Norris’ theory (Norris, 1996) that in order to minimise the variation in isotopic signal due to fractionation changes in foraminiferal growth and to establish consistent and reliable stable isotopic profiles, mass spectrometry experiments should be conducted in such a way as to ensure that the foraminiferal test samples used are of

the same size range.

We conclude that, despite the slightly different sampling resolution and the unavoidable problem that the number of foraminifera is not sufficient to control the size range of the selected tests, the data obtained from both mass spectrometers offer fully comparable records. These results confirm that, when equipped with a well-performing Gasbench peripheral and operated by trained and competent personnel, the relatively cheap Delta V Advantage mass spectrometer is perfectly suited to yield highly detailed and dependable results, similar to those obtained by means of much more expensive and complex instrumentations.

Table

Sample	Depth, m	initial weight, g	Dry weight, g	$\delta^{13}\text{C}$ vs VPDB, ‰	$\delta^{18}\text{O}$ vs VPDB, ‰	Quantity	Quality	Notes
CCR 771	-56.8	45.1	5.4678	-0.535341087	3.304678428	poor	good	Lots of sediment (quartz and mica).
CCR 772	-56.9	33.6	0.9323	-0.555476884	3.13501237	poor	good	
CCR 773	-57	45.5	1.2392	-0.535204109	3.2063127	poor	good	With some larger debris.
CCR 774	-57.1	43	6.5851	-0.46466033	3.360493133	poor	good	Lots of sediment (quartz and mica).
CCR 775	-57.2	44.8	1.2801	-0.445757338	3.226854803	poor	good	
CCR 776	-57.3	46.6	3.4561	-0.754780179	3.178561848	poor	good	Lots of sediment (quartz and mica).
CCR 777	-57.4	28.3	0.2509	-0.722727278	3.108825809	poor	good	
CCR 778	-57.5	41.4	0.3485	-0.571914269	3.163002975	poor	good	Many brown particles appear.
CCR 779	-57.6	43.5	0.7175	-0.739027685	3.155944392	poor	good	Many brown particles appear.
CCR 780	-57.7	48.8	0.2891	-0.692455094	3.194093675	poor	good	Many brown particles appear.
CCR 781	-57.8	48.5	1.8673	-0.433840233	3.155252534	poor	good	Many brown particles appear.
CCR 782	-57.9	48.6	0.7131	-0.346722092	3.035036602	poor	good	Many brown particles appear.
CCR 783	-58	46.3	0.9988	-0.345078353	2.915094086	poor	good	Many brown particles appear.
CCR 784	-58.1	50	11.9988	0.056130823	2.890289905	poor	good	Lots of sediment (quartz and mica).
CCR 785	-58.2	48.2	0.6811	-0.368912562	3.391001838	poor	good	Many brown particles appear.
CCR 786	-58.3	49.4	0.4976	-0.29480735	3.245988427	poor	good	Many brown particles appear.
CCR 787	-58.4	49.1	0.3417	-0.420553347	3.139607357	poor	good	Many brown particles appear.
CCR 788	-58.5	45.6	0.2643	-0.380418731	2.767040801	poor	good	Many brown particles appear.
CCR 789	-58.6	49.5	0.2813	-0.498630927	3.536481361	poor	good	Many brown particles appear.
CCR 790	-58.7	50.2	0.338			poor	good	Many brown particles appear.
CCR 791	-58.8	46.1	0.333	0.135304229	3.265970789	poor	good	Many brown particles appear.
CCR 792	-58.9	48.8	0.4237	-0.245769151	3.244527336	poor	good	Many brown particles appear.
CCR 793	-59	41.9	0.2754	-0.29480735	3.15814632	poor	good	Many brown particles appear.
CCR 794	-59.1	49.7	0.4585	-0.284260028	3.008882263	poor	good	Many brown particles appear.
CCR 795	-59.2	49.1	0.4746	-0.172622787	2.746181894	poor	good	Many brown particles appear.
CCR 796	-59.3	42	0.3736	-0.448222945	2.378538391	poor	good	Many brown particles appear.
CCR 797	-59.4	47.4	0.3483	-0.584927199	2.365512744	poor	good	Many brown particles appear.
CCR 798	-59.5	46.2	0.3527	-0.329188881	3.337007373	poor	good	Many brown particles appear.
CCR 798	-59.6	46.4	0.2372	-0.413704436	2.314063604	poor	good	Many brown particles appear.
CCR 799	-59.7	43.1	0.3136	-0.387267642	2.389614285	poor	good	Many brown particles appear.
CCR 800	-59.8	44.2	3.4139	-0.200429364	2.377895385	poor	good	Many brown particles appear.
CCR 801	-59.9	45.4	0.4447	-0.203716841	2.927335826	poor	good	Lots of sediment (quartz and mica).
CCR 802	-60	43.8	0.2988	-0.18769039	3.276481771	poor	good	Many brown particles appear.
CCR 803	-60.1	47.8	0.2687			poor	good	Significantly fewer brown particles
CCR 804	-60.2	41.3	0.2122	-0.267411708	3.12419334	poor	good	Brown particles disappear
CCR 805	-60.3	41.9	0.2916	-0.415074219	3.04178225	poor	good	
CCR 806	-60.4	45.3	0.4525			poor	good	
CCR 807	-60.5	46.6	0.5574	-0.283849093	3.018895133	present	good	
CCR 808	-60.6	47.6	0.3417	-0.554107102	3.038825505	poor	good	

CCR 809	-60.7	48.9	0.8148	-0.480549803	2.714189029	poor	good	
CCR 810	-60.8	49.2	0.3501	-0.32617536	2.667945318	poor	good	
CCR 811	-60.9	44.4	0.284	-0.420964282	2.64738524	poor	good	Brown particles appear.
CCR 812	-61	43.5	0.4254	-0.113037266	2.298768671	poor	good	Brown particles disappear.
CCR 813	-61.1	48.2	0.4124	-0.283712115	2.723889513	poor	good	
CCR 814	-61.2	40.6	0.3557	-0.450825531	2.484191225	poor	good	
CCR 815	-61.3	48.7	0.3974	-0.294944328	2.589202322	poor	good	
CCR 816	-61.4	44.3	0.4818	-0.605199974	2.507609445	poor	good	
CCR 817	-61.5	49.7	0.3135	-0.245221238	2.470881224	present	good	
CCR 818	-61.6	47.4	0.2756	-0.433703255	2.224055022	poor	good	
CCR 819	-61.7	46.1	0.3163	-0.501781425	1.979967821	poor	good	
CCR 820	-61.8	47.5	0.6592	-0.351242373	2.14156407	poor	good	
CCR 821	-61.9	45.1	0.4196	-0.322202992	1.71059434	poor	good	Many grey deposits appear.
CCR 822	-62	49.5	0.2107			poor	good	Fewer grey particles and white shell fragments appear.
CCR 823	-62.1	45	0.4067	-0.30631352	1.731543129	poor	good	
CCR 824	-62.2	46.7	0.3041	-0.223715659	1.792910351	poor	good	
CCR 825	-62.3	48.9	0.262	-0.517670898	1.779408041	poor	good	
CCR 826	-62.4	49.5	0.5189	-0.42795017	1.908808782	poor	good	
CCR 827	-62.5	48.8	0.3659			absent	Sapropel: Filled with two species of planktonic foraminifera.	
CCR 828	-62.6	47.5	0.5783			absent		
CCR 829	-62.7	38.4	0.3621			absent		
CCR 830	-62.8	45.1	5.4678			absent		

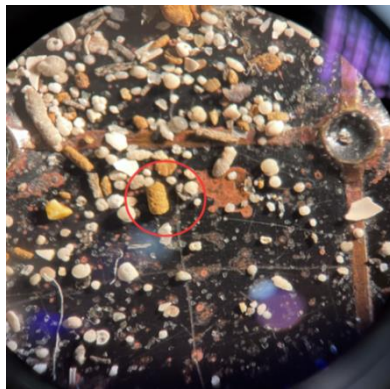


Figure a: brown particles observed in the samples (red circle).



Figure b: grey deposits observed in the samples.

## Acknowledgements

I would like to thank my supervisor Prof. Luca Capraro for his guidance and help with my dissertation, for always being patient and understanding of all my situations throughout the process of completing my experiments and dissertation, and also for his humour and witty classes that have given me a deeper interest and understanding of paleoceanography.

Many thanks also to Dr. Elena Zanola for helping me throughout the experiment and providing all the information I asked for, and for always keeping me warm with your every friendly greeting and wish.

I would also like to thank Dr. Carlotta Betto, Dr. Lisa Santello and Prof. Nereo Preto who provided guidance and assistance throughout the experiment.

There are also many thanks to Prof. Zattin, Prof. Ming Jin and Prof. Xiuxi Wang for their care and help throughout my studies in Italy.

Thank you to all the teachers, staff and schoolmates at the University of Padua, whom I know or don't know by name, for your kindness and enthusiasm.

Also, I am grateful to my parents, Ms Yuli Cai and Mr Lin, for supporting my study abroad during the most difficult financial times for my family and for always supporting me and believing in me.

Thank you to my grandmother, Mrs Chen, for being brave and positive in her fight against cancer, for always being upbeat and working hard and for constantly encouraging me to face any difficulties in my life, for keeping her alive with unimaginable willpower until I came home and calling my childhood name at the end of her life. I will always miss you and love you very much, Grandma.

Finally, thank you to my best friend, Wenxuan, for being there for me and supporting me throughout my study abroad experience in Italy.



## References

- ALTENBACH & SARNTHEIN, M., 1989. *Productivity record in benthic Foraminifera*, in Berger, W. H., Smetacek, V. S., & Wefer, G. (eds.). *Productivity of the Ocean: Present and Past*, John Wiley and Sons Ltd., New York, 255-269.
- ANDERSON, T.F. & ARTHUR, M.A., 1983. *Stable isotopes of oxygen and carbon and their application to sedimentologic and paleoenvironmental problems*. SEPM Society for Sedimentary Geology.
- BIGELEISEN, J., 1965. *Chemistry of isotopes*. *Science*, 147, 463-471.
- CAROBENE, L., 2003. *Genesis, age, uplift and erosion of the marine terraces of Crosia-Calopezzati (Ionian Coast of Calabria-Italy)*. *The Quaternary*, 16(1), 43-90.
- CUSHMAN, J.A., 1923. *The foraminifera of the Atlantic Ocean, Part 4. Lagenidae*. *Bulletin United States National Museum*, 104, 1-228.
- EMILIANI, C., 1955. *Pleistocene Temperatures*. *The Journal of Geology*.
- EMILIANI, C., 1966. *Paleotemperature analysis of the Caribbean Cores P6304-8 and P6304-9 and a generalised temperature curve for the last 425.000 years*. *Journal of Geology*, 74, 109-126.
- EPSTEIN, JR., BUCHSBACH, H.A., LOWENSTAM, & UKEY, .H.C., 1953. *Revised carbonate-water isotopic temperature scale*. *Bulletin of the geological society of America*, 64, 1315-1326.
- GASPERI, G., 1995. *Regional Geology*. Pythagoras Editions, Bologna, 464 pp.
- GAT, J.R., 1966. *Oxygen and hydrogen isotopes in the hydrologic cycle*. *Annual Review of Earth and Planetary Sciences*, 24, 225-262.
- GOZZER, L., 2011. *Depositional evolution of the Pleistocene basin of Calopezzati Crosia, (Cosenza, Calabria)*. Master's thesis in Nature Sciences, University of Padova.
- GRADSTEIN, F.M.M., OGG, J.G., SCHMITZ, M.B. & OGG, G.M., 2012. *The Geologic Time Scale 2012*. Elsevier Science, 115 pp.
- LOURENS, L.J., HILGEN, F.J., LASKAR, J., SHACKLETON, N.J. & WILSON, D., 2004. *The Neogene Period*. In: Gradstein, F.M., Ogg, J.G., Smith, A.G. (Editors), *A Geologic Time Scale 2004*. Cambridge University Press, Cambridge, 409-440.

LUZ, B., KOLODNY, Y., & KOVACH, J., 1984. *Oxygen isotope variations in phosphate of biogenic apatites. 3. Conodonts*. Earth and Planetary Science Letters, 69 (2), 255-262.

MASSARI, F., GHIBAUDO, G., D'ALESSANDRO, A. & DAVAUD, E., 2001. *Water-upwelling pipes and soft-sediment-deformation structures in lower Pleistocene calcarenites (Salento, southern Italy)*. Geological Society of America Bulletin, 113, 545-560.

MELANDER L., 1960. *Isotope Effects on Reaction Rates*. New York: Roland.

MILANKOVITCH, M., 1941. *Canon of Earth Irradiation and its Application to the ice age problem*. Royal Serbian Academy, Special Publication, 133, 633 pp.

NORRIS, R.D., 1996. *Symbiosis as an evolutionary innovation in the radiation of Paleocene planktic foraminifera*. Paleobiology, 22(4), 461-480.

OGNIBEN, L., 1962. *Flaky clays and Messinian sediments to the left of the Trionto (Rossano, Cosenza)*. Roman Geology, 1, 255-282.

POPP, B.N., ANDERSON, T.F., & SANBERG, P.A., 1986. *Brachiopods as indicators of original isotopic compositions in some Paleozoic limestones*. Geological Society of America Bulletin, 97 (10), 1262-1269.

RAYMO, M.E., RUDDIMAN, W.F., BACKMAN, J., CLEMENT, B.M. & MARTINSON, D.G., 1989. *Late Pliocene variations in the northern ice sheet and North Atlantic deep water circulation*. Paleoceanography, 4, 413- 466.

REGHELLIN, D., 2010. *Paleoclimatic and paleoenvironmental history of the Lower Pleistocene interval in the Crosia-Calopezzati Basin (Ionian Calabria, Southern Italy)*. Master's thesis in Nature Sciences, University of Padova.

SEGALLA, M., 2007. *Stratigraphic, chronological and palaeoenvironmental characterisation of the Pleistocene succession of Crosia-Calopezzati (Ionian Calabria)*. Master's thesis in Nature Sciences, University of Padova.

SHACKLETON, N.J., 1967. *Oxygen Isotope Analyses and Pleistocene Temperatures Re-assessed*. Nature, 215, 15-17.

SHACKLETON, N.J., 1977. *<sup>13</sup>C in Uvigerina: tropical rainforest history and the equatorial Pacific carbonate dissolution cycles*. In: Anderson, N., Malahof, A. (Editors), Fate of Fossil Fuel CO<sub>2</sub> in the Oceans Plenum, New York, 401- 427.

SHACKLETON, N.J., 1987. *Oxygen isotopes, ice volume and sea level*. Quaternary

Science Reviews, 6, 183-190.

SHACKLETON, N.J., AN, Z., DODONOV, A.E., GAVIN, J., KUKLA, G.J., RANOV, V.A. & ZHOU, L.P., 1995. *Accumulation rate of loess in Tajikistan and China: Relationship with global ice volume cycle*. Quaternary Proceedings, 4, 1-6.

SHACKLETON, N.J., HALL, M.A., LINE, J. & GANG, S., 1983. *Carbon isotope data in core VI9-30 confirm reduced carbon dioxide concentration of the ice age atmosphere*. Nature, 306, 319-322.

SHACKLETON, N.J. & OPDYKE, N.D., 1973. *Oxygen isotope and paleomagnetic stratigraphy of equatorial Pacific core V28-289: Oxygen isotope temperatures and ice volumes on a 105-year and 106-year scale*. Quaternary Research, 3, 39-55.

SHACKLETON, N.J. & OPDYKE, N.D., 1976. *Oxygen-isotope and paleomagnetic stratigraphy of Pacific core V28-239, late Pliocene to latest Pleistocene*. Geological Society of America, Memoir, 145, 449- 464.

SHEEPERS, P.J.J., 1994. *Tectonics rotations in the Tyrrhenian Arc system during the Quaternary and Late Terziary*. Geological Ultraiectin, 112, 350 pp.

STRÖHLE, K. & KROM, M.D., 1997. *Evidence for the evolution of an oxygen minimum layer at the beginning of S-1 sapropel deposition in the eastern Mediterranean*. Marine Geology, 140, 231-236.

UREY, H.C., 1947. *The thermodynamic properties of isotopic substances*. Journal of Chemical Society, 562-581.

UREY, H.C., 1948. *Oxygen Isotopes in Nature and in the Laboratory*. Science, 2810, 489-496.

UREY, H.C., LOWENSTAM, H.A., EPSTEIN, S., & MCKINNEY, C.R., 1951. *Measurement of paleotemperatures and temperatures of the upper Cretaceous of England, Denmark, and the southeastern United States*. Geological Society of America Bulletin, 62, 399-416.

VAN DIJK, J.P., 1992. *Late Neogene fore-arc basin evolution in the Calabrian Arc (Central Mediterranean); tectonic sequence stratigraphy and dynamic geohistoty. With special reference to the geology of Central Calabrian*. Geological Ultraiectin, 92, 288 pp.

VAN DIJK, J.P., 1993. *Three-dimensional quantitative restoration of Central Mediterranean Neogene basin*. In: Spencer A.M. (Editor), *Generation, accumulation and production of Europe's hydrocarbons III*. Special publication, European

Association of Petroleum Geologists, 3, 267-280.

VAN DIJK, J.P & OKKES M., 1991. *Neogene tectono stratigraphy and kinematics of Calabrian basin; implication for the geodynamics of the Central Mediterranean*. Tectophysics, 196, 23-60.

VAN DIJK, J.P & SHEEPERS, P.J.J., 1995. *Neotectonic rotations in the Calabrian Arc; implication for a Pliocene Recent geodynamics scenario for the Central Mediterranean*. Earth Science Reviews, 39, pp. 207-246.

WANG, W., 2023. *Changes in biological productivity in the lower part of the PCS sediment core (Lower Pleistocene, Calabria, Southern Italy)*. Master's thesis in Nature Sciences, University of Padova.

WEISS, R. S.,1973. *The experience of emotional and social isolation*. The MIT Press.